No More Than Three: Technoeconomic Mixed Integer Nonlinear Programming Optimization of Mixed Suspension, Mixed Product Removal Crystallizer Cascades for Melitracen, an Antidepressant API

No More Than Three: Technoeconomic Mixed Integer Nonlinear Programming (MINLP) Optimization of Mixed Suspension, Mixed Product Removal (MSMPR) Crystallizer Cascades for Melitracen, an Antidepressant API

Samir Diab, Dimitrios I. Gerogiorgis*

Institute for Materials and Processes (IMP), School of Engineering, University of Edinburgh, The Kings Buildings, Edinburgh, EH9 3FB, Scotland, UK

**Corresponding Author*: *D.Gerogiorgis@ed.ac.uk*

ABSTRACT

Mixed Suspension, Mixed Product Removal (MSMPR) crystallizers have been considered in numerous cases as a continuous mode of operation in the production of Active Pharmaceutical Ingredients (APIs). The steady-state continuous MSMPR crystallization of melitracen via cooling has been recently demonstrated in the literature, with crystallization kinetic parameters regressed from experimental data. Mixed Integer Nonlinear Programming (MINLP) has been implemented extensively for the optimization of separation process designs in various manufacturing sectors, but not for systematic design and screening of MSMPR cascade flowsheet configurations. This study performs MINLP optimization to maximize the Net Present Value (NPV) of a MSMPR cascade for continuous melitracen crystallization with solids recycle. Process flowsheets consider varying numbers of crystallizers and recycle stream feed point location. First, the MSMPR model describing API solubility, crystallization kinetics, population balance equations and process mass balances are described. The MINLP problem and constraints are then described with detailed costing equations. The optimal flowsheet configuration for both considered plant capacities (10^3 and 10^4 kg API yr^{-1}) is three crystallizers with recycle fed to the first and last vessels. This study illustrates the utility of rapid screening of continuous crystallization cascades via MINLP optimization to facilitate process development towards fully Continuous Pharmaceutical Manufacturing (CPM) plant designs.

1. Introduction

Continuous crystallization is an emerging field of research due to its potential to enhance process flexibility, efficiency and product quality consistency compared to batch techniques.[1] Development of robust continuous crystallizer designs is imperative for Continuous Pharmaceutical Manufacturing (CPM) campaigns, which have received significant attention from academic, industrial and regulatory bodies in the past decade.[2–4] Crystallization is a key unit operation in pharmaceutical manufacturing given the predominance of solid dosage forms in pharmaceutical products. Implementation of robust control mechanisms for control of particulate process operation in pharmaceutical production is required to meet stringent product requirements inherent of Drug Product (DP) formulations, which also affect drug bioavailability.[5–7] Mixed Suspension, Mixed Product Removal (MSMPR) crystallizers are a widely studied continuous design for their simple operation, low maintenance requirements, avoidance of rapid fouling typical of continuous tubular designs and ease of adaptation from existing batch stirred tank designs.[8]

A variety of experimental and theoretical studies have already investigated the design, simulation and optimization of steady-state and dynamic operations of MSMPR crystallizers for different Active Pharmaceutical Ingredients (APIs) and other pharmaceutically relevant compounds.[9] Recent work regarding comparison operating strategies, process configurations and control,[10–19] novel crystallization techniques,[20–23] configurations with filtration and recycle,[11,24–27] enantiomeric and chiral molecule separation[28–30] and polymorph selectivity[31,32] have significantly developed MSMPR implementation, with some designs integrated into end-to-end CPM plants.[33] Intensification of MSMPR crystallization by incorporation of size control processes such as we milling have also received interest.[34,35] Rapid screening of candidate flowsheet configurations of MSMPR cascades for different APIs can facilitate process development towards end-to-end CPM.[3,36]

Melitracen is a tricyclic antidepressant API available as single drug preparations and also in combinative therapies.[37] The number of US citizens affected by depression and of defined daily doses of antidepressants distributed in the UK have been historically increasing (Fig. 1).[38,39] The continuous crystallization of the API in MSMPR crystallizers was recently demonstrated,[40] facilitating its process modelling and optimization. Existing studies investigate the effects of MSMPR design and operating parameters on crystal size, showing significant variation in process performance and crystal product attributes when varying the number of implemented crystallizers.[7] Investigating the effect of longer cascades and recycle options can further improve crystallization yields in MSMPR design.[11] Economic considerations are equally important as meeting specific product attribute targets when designing crystallization processes, especially when the effect of production scale is considered.[36,41,42]

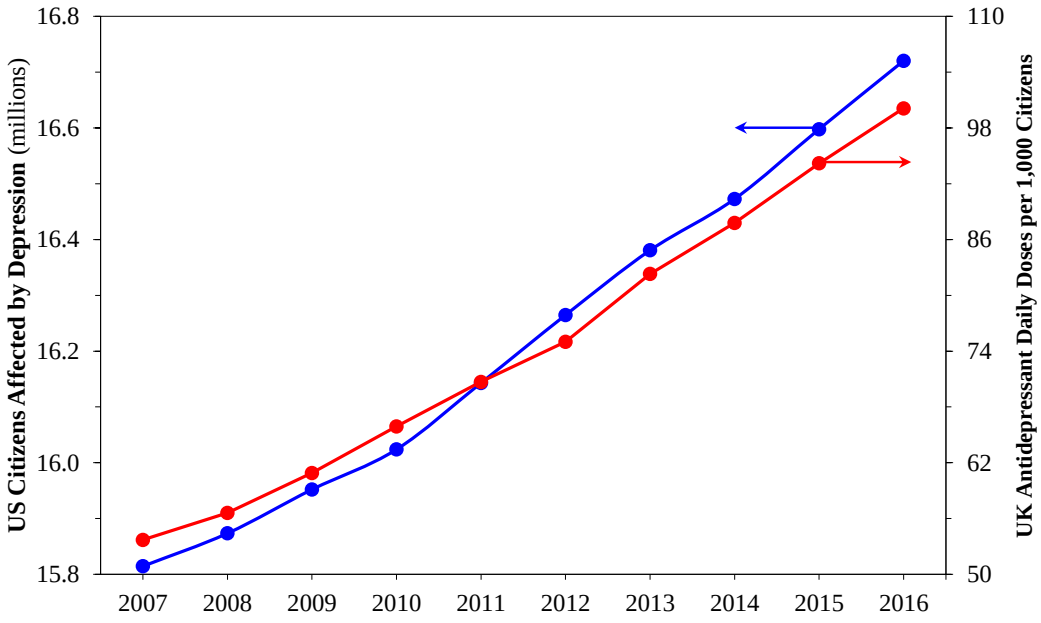

Figure 1: Historical trends in number of US citizens affected by depression[43] and number of defined daily dosages administered per 1,000 UK inhabitants.[44]

Mixed Integer Nonlinear Programming (MINLP) has been widely implemented in various applications to rapidly screen for optimal design configurations of separation processes. Optimization of distillation column trains,[45–47] adsorption cycles,[48,49] Liquid-Liquid Extraction (LLE) cascades,[50,51] chromatographic resolutions[52] and membrane separations[53–55] have been covered extensively in the literature, showing promise of significant process improvements via MINLP optimization. Mixed integer problems contain both continuous decision variables, e.g., unit operating and design parameters, as well as integer (binary or otherwise) decision variables, e.g., denoting the existence of a unit operation or deciding stream allocation.

Various NLP problems have been considered in the literature for different continuous crystallization processes, objectives and constraints. Su et al. (2015) described the design of a two-stage MSMPR crystallization cascade, maintaining the process within the design space of a specified batch design.[8] The MSMPR process design attained a higher yield and production capacity than the batch alternative, but a lower mean crystal size. Vetter et al. (2014) established attainable regions of particle sizes vs. residence time subject to constraints on yield, operating temperature and antisolvent feed rate in MSMPR and plug flow crystallizers; subsequent minimization of the residence time for a given process configuration gave optimum process designs for comparative evaluation.[15]

Li et al. (2017) solved a NLP problem for maximum yield subject to purity constraints and maximum purity subject to yield constraints for MSMPR cooling crystallization cascades.[23] Other studies address optimization in plug flow crystallizers where multi-objective optimization problems were solved for antisolvent allocation to different tube segments to maximize mean product size and minimize size distribution width.[56,57]

These NLP studies mainly address continuous crystallization optimization with respect to product size properties and purity. These studies do not consider process economics or production capacity specifications. Optimization of MSMPR cascades with economic NLP objective functions has been previously demonstrated,[36] but do not consider process synthesis to optimality or solids recycle options. Therein lies the novelty and aim of this study – the formulation of a MINLP problem for MSMPR cascade synthesis with optimal recycle stream allocation for economic optimization comparing different numbers of crystallizers and plant capacities. Optimization of MSMPR cascades using MINLP has yet to be implemented and may be a valuable tool for rapid design and flowsheet configuration screening.

This study implements MINLP optimization of a MSMPR cascade for continuous melitracen crystallization to screen for cost optimal flowsheet configurations. The MINLP superstructure for MSMPR cascades considers varying crystallizer volumes, extent of recycle, concentration of recycle streams and their allocation to different MSMPR vessels. The steady-state process model describes the crystallization process by simultaneous solution of crystallization kinetics, population balances and mass balance equations. The MINLP problem is solved for different plant capacities. Optimal total cost components (with sensitivity analysis), unit operation design, flowsheet configurations, crystallization yields and mean crystal sizes are compared for different problem instances.

2. MSMPR Crystallization Model

The considered steady-state MSMPR model makes the following assumptions:

1. The fresh feed stream to the process is a homogeneous mother liquor containing dissolved API and no crystals. Crystallizers are not seeded.
2. Crystal birth occurs by nucleation only and growth only occurs in one characteristic dimension.
3. Growth is size-independent and there is no agglomeration, crystal breakage or attrition.
4. The contents of the crystallizer are perfectly mixed, i.e., the supersaturation field in the crystallizer is uniform, and the product magma has the same composition as the crystallizer contents.
5. Crystallization occurs only within the MSMPR vessels and not in connecting or recycle streams.

All flowsheets and process designs are for plant API capacities of $Q_{API} = \{10^3, 10^4\}$ kg API yr^{-1}. The steady-state process model for all flowsheet configurations describe crystallization kinetics, population balance equations and mass balances. Simultaneous solution of these equations describes continuous crystallization in the MSMPR crystallizer cascade.

2.1 Process Flowsheets

Capellades et al. (2019) demonstrated continuous crystallization of melitracen from ethanol via cooling in a MSMPR cascade without recycle.[40] Solids recycling in MSMPR cascades has been demonstrated in the literature, allowing for enhanced crystallization yields.[11,58] In this study, we model and optimize a MSMPR cascade with solids recycle, whose process flowsheet is illustrated in Fig. 2.

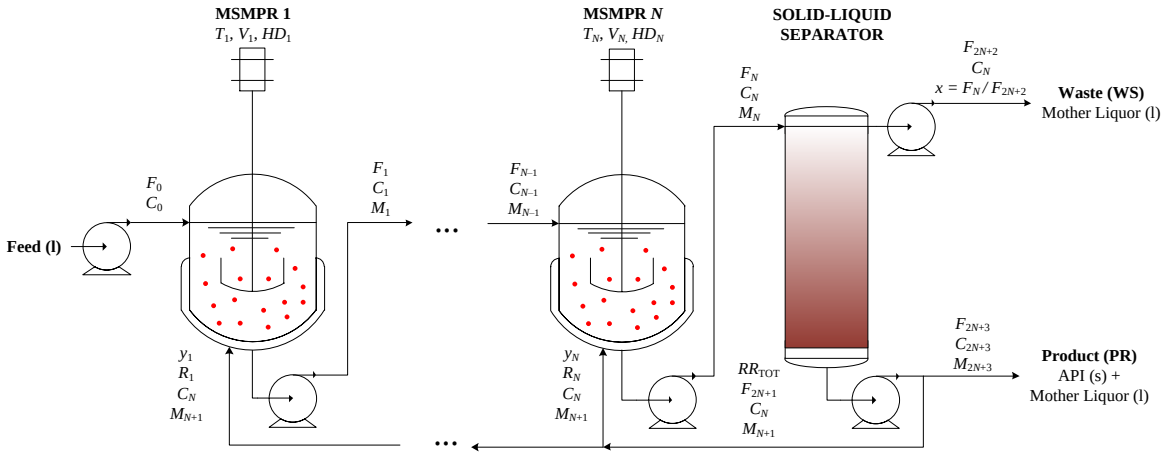

Figure 2: MSMPR cascade for continuous crystallization with solids recycle.

A clear mother liquor feed stream enters MSMPR 1, with dissolved API solute concentration C_0 and volumetric flowrate F_0. The feed mother liquor solution containing melitracen has concentration, C_0 = 129.5 g L^{-1}, as per the experimental demonstration.[40] The product stream exiting one MSMPR (F_i) is then the feed stream to the subsequent MSMPR in the cascade, consisting of N crystallizers in total.

The product stream of crystallizer N (F_N) then enters a solid-liquid separator, in which clear mother liquor is removed (F_{2N+2}) in order to concentrate the stream suspension, which exits from the bottom of the separator, producing recycle streams R_i. The concentrated stream is the product (F_{2N+3}), with some being recycled back to select crystallizers.

Design and operating parameters for the process are the MSMPR temperatures (T) and volumes (V), the total recycle ratio (RR_{TOT}), the mother liquor removal ratio ($x = F_N / F_{2N+2}$) and binary variable, y_i, deciding whether to send recycle to stage i. Each MSMPR i has a holdup of crystallized API, HD_i. For each crystallizer, F_i, C_i and M_i are the volumetric flowrate of the stream leaving the stage, the equilibrium API concentration in the mother liquor and the suspension density, respectively.

2.2 API Solubility

The solubility concentration of API in ethanol, C^{sat}, as a function of temperature during cooling crystallization is described by eq. 1, taken from the literature, with a coefficient of determination, $R^2 > 0.99$ vs. experimental data.[40] The published experimental data and the regressed correlation (eq. 1) of C^{sat} vs. T are shown in Fig. 3. No polymorphism under the considered temperature ranges was described in the experimental study on MSMPR cooling crystallization of melitracen from ethanol and so polymorphic effects are not considered here.[40]

$$C_i^{sat} = 15.282 \exp(0.041 T_i) \qquad \forall i = 1,\ldots,N \tag{1}$$

2.3 Crystallization Kinetics

Crystal nucleation, B, and growth, G, rates are expressed via eqs. 2 and 3, respectively.

$$B_i = k_{b0} \exp\left(-\frac{E_b}{R(T_i + 273.15)}\right)\left(\frac{C_i}{C_i^{sat}} - 1\right)^b M_i^m \qquad \forall i = 1,\ldots,N \tag{2}$$

$$G_i = k_{g0} \exp\left(-\frac{E_g}{R(T_i + 273.15)}\right)\left(\frac{C_i}{C_i^{sat}} - 1\right)^g \qquad \forall i = 1,\ldots,N \tag{3}$$

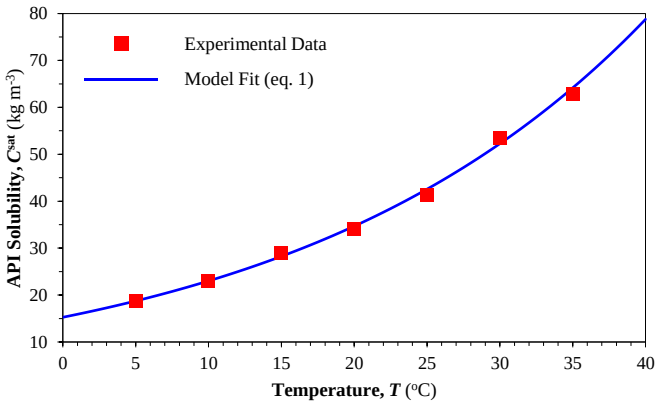

Figure 3: Melitracen solubility concentration (C^{sat}) as a function of temperature (T) in ethanol vs. experimental data ($R^2 > 0.99$).[40]

Here, k_{b0} and k_{g0} are nucleation and growth pre-exponential factors, E_b and E_g are energy barriers to nucleation and growth, respectively, R is the universal gas constant, b and g are nucleation and growth exponents, respectively, and m is the suspension density exponent. All crystallization kinetic parameters are listed in Table 1.

2.4 Population Balance Equations

The general one-dimensional population balance model is described by a system of Ordinary Differential Equations (ODEs). For a MSMPR cascade with slurry recycle, the population balance equations are described by eqs. 4–6. Here, n_i is the population density function of crystals between size L and L+dL. In eq. 5, the first term represents the stream entering from the previous stage (i–1), the second term represents the recycle stream entering stage i and the last term represents the product stream leaving stage i. Eqs. 4–6 form a system of ODEs that are satisfied by the boundary conditions, n_i^0 (eq. 6), representing the population density of nuclei.

$$G_1 V_1 \frac{\mathrm{d}n_1}{\mathrm{d}L} = R_1 n_{N+1} - F_1 n_1 \tag{4}$$

$$G_i V_i \frac{\mathrm{d}n_i}{\mathrm{d}L} = F_{i-1} n_{i-1} + R_i n_{N+i} - F_i n_i \qquad \forall i = 2,\ldots,N \tag{5}$$

$$n_i^0 = \frac{B_i}{G_i} = n_i(L=0) \qquad \forall i = 1,\ldots,N \tag{6}$$

The suspension density, M_i, is calculated from the population balance via eq. 7. Here, k_v and ρ_{API} are the volume shape factor and crystal density of API solute; values for these are provided in Table 1.

$$M_i = k_v \rho_{API} \int n_i L^3 \mathrm{d}L \tag{7}$$

Table 1: Kinetic parameters for MSMPR crystallization of melitracen from ethanol.[40]

Model Equations	Parameter	Value	Units
Nucleation rate, B	k_{b0}	4.79×10^{22}	m^{-3} s^{-1}
(eq. 2)	E_b	7.30×10^{4}	J mol^{-1}
	b	2.60	(–)
	m	0.56	(–)
Growth rate, G	k_{g0}	13.1	m s^{-1}
(eq. 3)	E_g	5.25×10^{4}	J mol^{-1}
	g	0.87	(–)
Population balances	k_v	3.74	(–)
(eqs. 4–6)	ρ_{API}	1,280	kg m^{-3}

2.5 Mass Balances

The steady-state mass balances for each process assume no material accumulation and account for volumetric changes due to API crystallization. The general mass balance equations for processes are:

$$F_0 C_0 + F_{N+1}\left(1 - \frac{M_{N+1}}{\rho_{\text{API}}}\right) C_N + R_1 M_{N+1} - F_1\left(1 - \frac{M_1}{\rho_{\text{API}}}\right) C_1 - F_1 M_1 = 0 \tag{8}$$

$$F_{i-1}\left(1 - \frac{M_{i-1}}{\rho_{\text{API}}}\right) C_{i-1} + F_{i-1} M_{i-1} + R_i\left(1 - \frac{M_{N+1}}{\rho_{\text{API}}}\right) C_N + R_i M_{N+1} - F_i\left(1 - \frac{M_i}{\rho_{\text{API}}}\right) C_i - F_i M_i = 0 \qquad \forall i = 2,\ldots,N \tag{9}$$

Eq. 8 describes stage 1 in the MSMPR cascade. The first term in eq. 8 is the dissolved API in the feed mother liquor stream to the cascade, the second and third terms are the API dissolved in the mother liquor and crystallized API in the recycle stream fed to stage 1, respectively, and the third and fourth terms are the API dissolved in the mother liquor and crystallized API leaving stage 1, respectively. Eq. 9 describes MSMPR stages $i = 2,...,N$, whose terms are similar to eq. 8 but without the fresh feed mother liquor term (F_0C_0). In both eqs. 8 and 9, the bracketed terms describe the volume fraction of the suspension not occupied by crystallized API.

It is assumed that the total stream of recycled material (F_{2N+1}) is equally distributed between those crystallizers to which it will be fed (i.e., those with binary variable $y_i = 1$). A mass balance equation around the gravity-driven solid-liquid separator gives the following.

$$M_{N+1} = \frac{M_N}{(1 - x)} \tag{10}$$

$$R_i = \frac{y_i RR_{\text{TOT}}(1 - x)}{\sum_{i=1}^{N} y_i} F_N \qquad \forall i = 1,\ldots,N \tag{11}$$

Here, x is the clear liquor removal ratio (controlling the suspension density of the stream leaving the bottom of the solid-liquid separator, M_{N+1}), defined as F_N / F_{2N+2} (see Fig. 2) and RR_{TOT} is the total recycle ratio (controlling how much is sent back to the MSMPR cascade vs. that withdrawn as product).

2.6 Crystallization Yield

The crystallization yield in MSMPR i is calculated from the equilibrium API concentration (C_i) in the mother liquor compared to that of the fresh feed stream (C_0).

$$Y_i^{\text{cryst}} = 100\left(1 - \frac{F_i C_i}{F_0 C_0}\right) \qquad \forall i = 1,\ldots,N \tag{12}$$

2.7 MSMPR Model Solution Method

Simultaneous solution of the MSMPR model (eqs. 1–11) requires iteration on the vector of C_i values, where $C_0 > C_i > C_i^{\text{sat}}$. Fig. 4 illustrates the workflow for the simultaneous solution of eqs. 1–11.[58,59] First, an initial guess is made for C_i values. The suspension densities are then estimated by solution of the mass balance equations, M_i^{mb}. Crystallization kinetics are then computed, allowing solution of the system of ODEs describing population balances. Suspension densities via the population balance equations, M_i^{pbe}, are then calculated. If the difference between M_i^{mb} and M_i^{pbe} is greater than the set tolerance (= 10^{-6}), another guess of C_i values are made. Upon convergence, the system of MSMPR model equations is solved and cost components are calculated (described in sections 3.1 and 3.2).

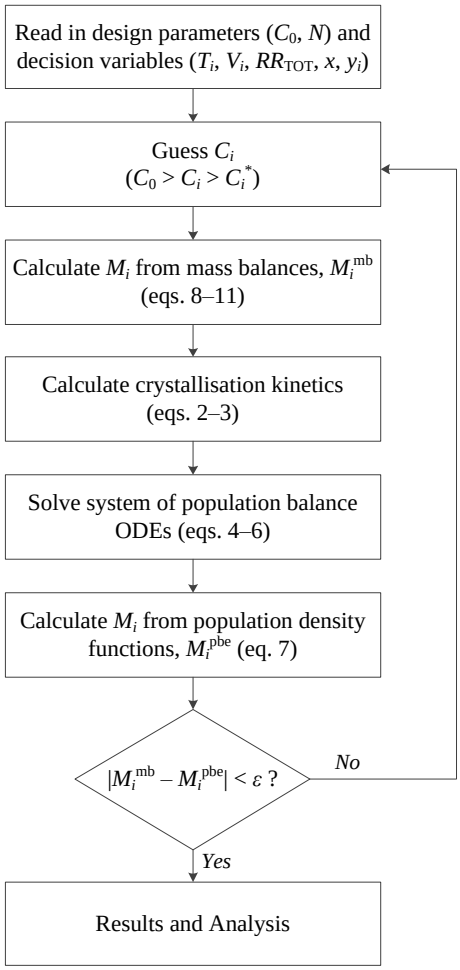

Figure 4: Algorithm for simultaneous solution of the MSMPR crystallization model.

3. MINLP Optimization Problem Formulation

3.1 Objective Function and Constraints

The objective of the MINLP optimization problem is to maximize the attained Net Present Value (*NPV*) of the crystallization process (eq. 13). The problem has $2N+2$ continuous decision variables (V_i, T_i, x, RR_{TOT}) and N binary variables (y_i). Various constraints are imposed on the problem. Crystallizer volumes must be finite (eq. 14). Temperatures are bounded such that the solubility estimation (eq. 1) is consistent with experimental results in the literature[40] (eq. 15). For cooling crystallization, each MSMPR temperature must be equal to or lower than the previous (eq. 16) and the fresh feed mother liquor is at $T_0 = 60$ °C (eq. 17), as per the experimental demonstration.[40] The total recycle ratio (RR_{TOT}) and clear solvent removal ratio (x) are constrained to values observed in the literature[11] (eqs. 18 and 19). Binary decision variables must be 0 or 1 (eq. 20). The considered plant capacity (Q_{API}) is also specified as a constraint by ensuring that crystallization process efficiencies and stream flowrates are such that the required amount of solid API is produced in the product stream (F_{2N+3} in Fig. 2).

$$\max NPV \tag{13}$$
$$0 < V_i \qquad \forall i = 1,\ldots,N \tag{14}$$
$$0 \leq T_i \leq 40\ °C \qquad \forall i = 1,\ldots,N \tag{15}$$
$$T_N \leq \ldots \leq T_1 \qquad \forall i = 1,\ldots,N \tag{16}$$
$$T_0 = 60\ °C \tag{17}$$
$$0.0 \leq RR_{TOT} \leq 0.9 \tag{18}$$
$$0.0 \leq x \leq 0.5 \tag{19}$$
$$y_i = \{0,1\} \qquad \forall i = 1,\ldots,N \tag{20}$$
$$F_{2N+3} M_{2N+3} = Q_{API} \tag{21}$$

3.2 Costing Methodology

This section describes the costing methodology implemented for calculation of the MINLP optimization objective function (eq. 13), *NPV*. The costing methodology is used in numerous studies on continuous manufacturing and API crystallizations and is described in detail herein.[41]

3.2.1 Capital Expenditure (CapEx)

All plant designs are assumed to be constructed and operated at an existing pharmaceutical manufacturing site with essential auxiliary structures already in place. Annual operation of 8,000 hours is considered.

Prices for equipment of similar capacities to those considered here have been sourced where possible; where such data is unavailable, the following cost-capacity correlation is used.

$$P_{\mathrm{B}} = f P_{\mathrm{A}} \left(\frac{S_{\mathrm{B}}}{S_{\mathrm{A}}}\right)^{n} \tag{22}$$

Here, P_j is the equipment purchase cost at capacity S_j. Parameters n and f are equipment-dependent and found in the literature.[60] Where the reference purchase cost (P_{A}) is taken from the past, Chemical Engineering Plant Cost Indices (CEPCIs) are used to calculate the corresponding purchase cost in the present. All capacities are scaled to account for process inefficiencies and to meet the specified plant capacity (Q_{API}). Unit operations similar to those implemented in the demonstrated continuous crystallization were scaled and costed using published eq. 22 parameters; Table 2 details the purchase costs and parameters in eq. 22 for each equipment item. The number of units for each item is also shown in Table 2; the number of crystallizers = N, there are N pumps (one per crystallizer outlet), one for the fresh feed entering the cascade, one for the mother liquor removed from the top of the separator and one for the concentrated slurry exiting the bottom of the separator, i.e., N+3 pumps in total.

Table 2: Parameters for scaled equipment purchase costs (eq. 22).[60]

Item	Ref. Year	Ref. Cost, P_{A} (GBP)	Capacity Basis	Ref. Capacity, S_{A}	n	f (%)	No. Items
Crystallizer	2007	328,875	m^3	3.00	0.53	10.33	N
Pump	2015	958	(–)	(–)	1.00	(–)	N+3
Separator	2007	207,900	L s^{-1}	58	0.64	10.33	1

The sum of all inflation-adjusted equipment costs (P_{B}) gives the Free-on-Board (*FOB*) cost. The Chilton method is used to calculate the Battery Limits Installed Cost (*BLIC*).[61] The Installed Equipment Cost (*IEC*), Process Piping and Instrumentation (*PPI*) and Total Physical Plant Cost (*TPPC*) are calculated via eqs. 23–25. A construction factor of 30% is added to the *TPPC* to calculate the *BLIC* (eq. 26).

$$IEC = 1.43FOB \tag{23}$$
$$PPI = 0.42IEC \tag{24}$$
$$TPPC = IEC + PPI \tag{25}$$
$$BLIC = 1.3TPPC \tag{26}$$

Working Capital (*WC*) costs are 3.5% of annual material costs (MAT_{annual}) (eq. 27). Contingency Costs (*CC*) are calculated as 20% of the *BLIC* (eq. 28). The sum of *BLIC*, *WC* and *CC* gives the total Capital Expenditure (*CapEx*, eq. 29).[41]

$$WC = 0.035MAT_{\mathrm{annual}} \tag{27}$$
$$CC = 0.2BLIC \tag{28}$$
$$CapEx = BLIC + WC + CC \tag{29}$$

3.3.2 Operating Expenditure (OpEx)

The annual utilities cost ($UTIL_{annual}$) is calculated as 0.96 GBP kg^{-1} of process material throughput ($m_{process}$) + crystallizer jacket cooling (Q_{MSMPR}), assuming an electricity consumption rate of 0.136 GBP kWh^{-1} (η) and an assumed conservative value of electricity efficiency of 40%. The annual waste cost ($Waste_{annual}$) is 0.35 GBP L^{-1} of waste (Q_{waste}). Annual Operating Expenditure ($OpEx_{annual}$) is the sum of annual material, utilities and waste costs.[41]

$$UTIL_{annual} = 0.96 m_{process} + \eta \Sigma Q_{MSMPR,i} \quad (30)$$

$$Waste_{annual} = 0.35 Q_{waste} \quad (31)$$

$$OpEx_{annual} = MAT_{annual} + UTIL_{annual} + Waste_{annual} \quad (32)$$

3.2.3 Net Present Value (NPV)

The Net Present Value (*NPV*) is calculated as the sum of inflation-adjusted profit from API sales minus *OpEx* over the plant lifetime minus total *CapEx* (eq. 33). Annual profit is calculated from sales of API produced (eq. 34). The wholesale price of melitracen (p_{API}) is taken as 50 GBP kg API^{-1}.

$$NPV = -CapEx + \sum_{k=1}^{t} \frac{\text{Profit} - OpEx_{annual}}{(1+r)^k} \quad (33)$$

$$\text{Profit} = p_{API} Q_{API} \quad (34)$$

A plant-operating lifetime of t = 20 yr and a base case interest rate of r = 5% are considered. All *CapEx* is assumed to occur in year 0 and operation is assumed to begin in year 1. Annual operation of 8,000 hours per year is assumed for consistency with our previously published work in this field. The assumed annual operation time can easily be altered to account for varying asset utilization efficiencies in the presented modelling framework.

3.3 Problem Structure and Solution Method

The problem is solved for separate instances of N = {1, 2, 3, 4, 5}. The problem has $2N$+2 continuous decision variables (V_i, T_i, x, RR_{TOT}) and N binary variables (y_i). For each problem instance, there are varying numbers of decision variables and constraints. There are $4N$+4 continuous linear inequality constraints (upper and lower bounds on each continuous decision variable) and $2N$ binary variable linear inequalities (respective upper and lower bounds). Table 3 shows the number of decision variables and constraints for different problem instances (i.e., N) considered.

Table 3: Number of decision variables for different problem instances (i.e., different N).

	Type	***N***	**1**	**2**	**3**	**4**	**5**
Variable	Continuous	V_i	1	2	3	4	5
		T_i	1	2	3	4	5
		RR_{TOT}	1	1	1	1	1
		x	1	1	1	1	1
	Binary	y_i	1	2	3	4	5
		Total	5	8	11	13	17
Constraint	Linear Inequality	V_i	2	4	6	8	10
		T_i	2	4	6	8	10
		RR_{TOT}	2	2	2	2	2
		x	2	2	2	2	2
		y_i	2	4	6	8	10
		Total	10	16	22	28	34

The MINLP problem is solved for separate instances of N and plant capacity Q_{API} = {10^3, 10^4} kg API yr^{-1} using the Basic Open-source Nonlinear Mixed Integer (BONMIN) solver in MATLAB's OPTI Toolbox.[62] The solver uses a branch and bound algorithm, where the relaxed Mixed Integer Linear Programming (MILP) problem solutions at each node of the MINLP search tree are replaced by relaxed

Nonlinear Programming (NLP) solutions, which are then solved via the Interior Point Nonlinear Optimizer (IPOPT) solver.[63] A multistart routine using multiple initial guesses for each decision variable is also implemented.

5. Results and Discussion

The results are presented as follows. First, crystallization kinetics, supersaturations and suspension densities resulting from optimization of the MINLP problem and their effect on resulting Mean Crystal Sizes (*MCS*) are discussed. Optimal flowsheet configurations, crystallizer volumes (*V*), operating temperatures (*T*) and recycle assignment (RR_{TOT}, *x*, *y*) are then presented for different plant capacities (Q_{API}) and numbers of crystallizers (*N*). Resulting crystallization yields and plantwide unit material efficiencies are then shown. A detailed cost breakdown of optimal total cost components and resulting maximum *NPV* values for different designs followed by a sensitivity analysis on assumed interest rate (*r*) for cost optimal designs are then presented.

5.1 Crystallization Kinetics and Mean Crystal Sizes

Crystallization kinetics (nucleation and growth rates, *B* and *G*, respectively) for different plant capacities (Q_{API}) and number of crystallizers (*N*) are shown in Fig. 5. The system of model equations for crystallization kinetics, mass balances and population balances are solved simultaneously to describe the MSMPR cascade behaviour. Growth rates increase along the cascade until $N = 3$ and then decrease, while nucleation rates generally continually increase and then plateau. The balance of growth and nucleation rates in a crystallization system is important in controlling the crystallization yield (affecting the process efficiency and resulting cost components) and product quality attributes such as *MCS* and size distribution width (affecting downstream operations and drug bioavailability). The crystallization kinetics and population balance equations assume 1D growth and primary nucleation only. Explicit secondary nucleation kinetics included in the model will enhance the model fidelity and deepen understanding of the considered process.

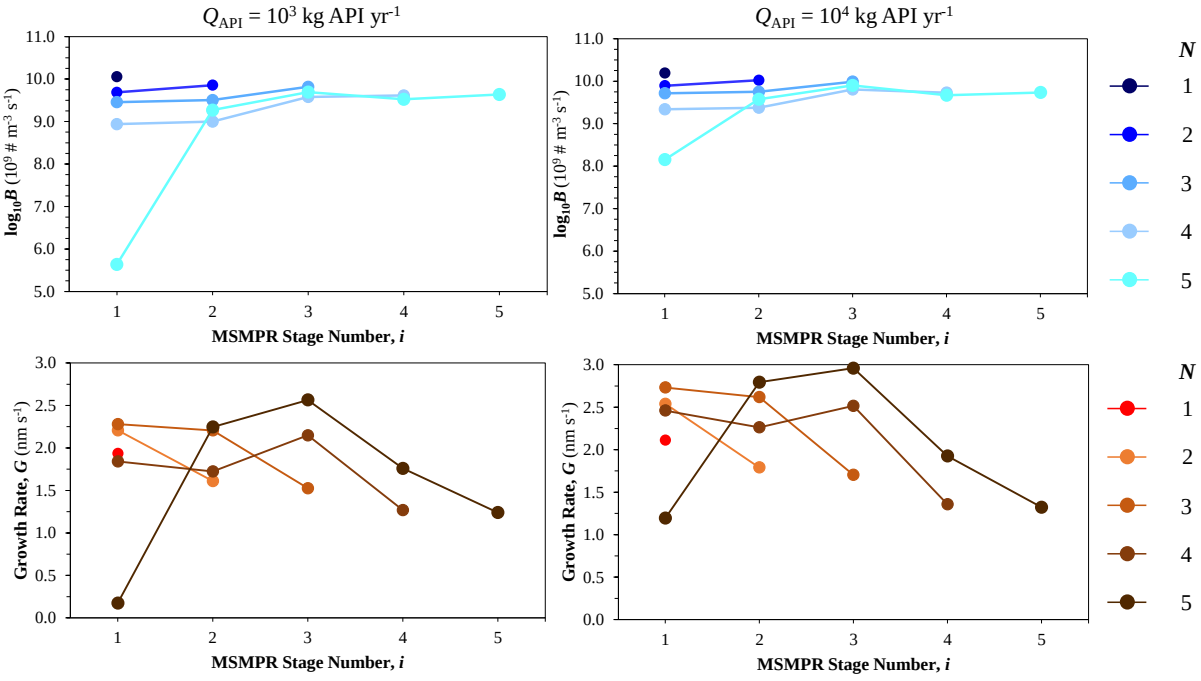

Figure 5: Optimal crystal nucleation (*B*) and growth (*G*) rates at both considered plant capacities (Q_{API}) at each stage (*i*) for different assumed numbers of crystallizers (*N*).

Resulting supersaturations and suspension densities (*M*) for different considered plant capacities (Q_{API}) and number of crystallizers (*N*) are shown in Fig. 6. The supersaturation gradually increases along the MSMPR cascade in all design cases with decreasing temperature (see Fig. 10, section 5.2). Suspension densities (*M*) increase continually along the cascade in all cases as the crystallization yield,

and hence amount of solid product in suspension, increases. The chosen upper bound of the clear mother liquor removal ratio (x) in the MINLP problem definition is such that suspension densities are not so high that streams cannot be handled by peristaltic pumps.

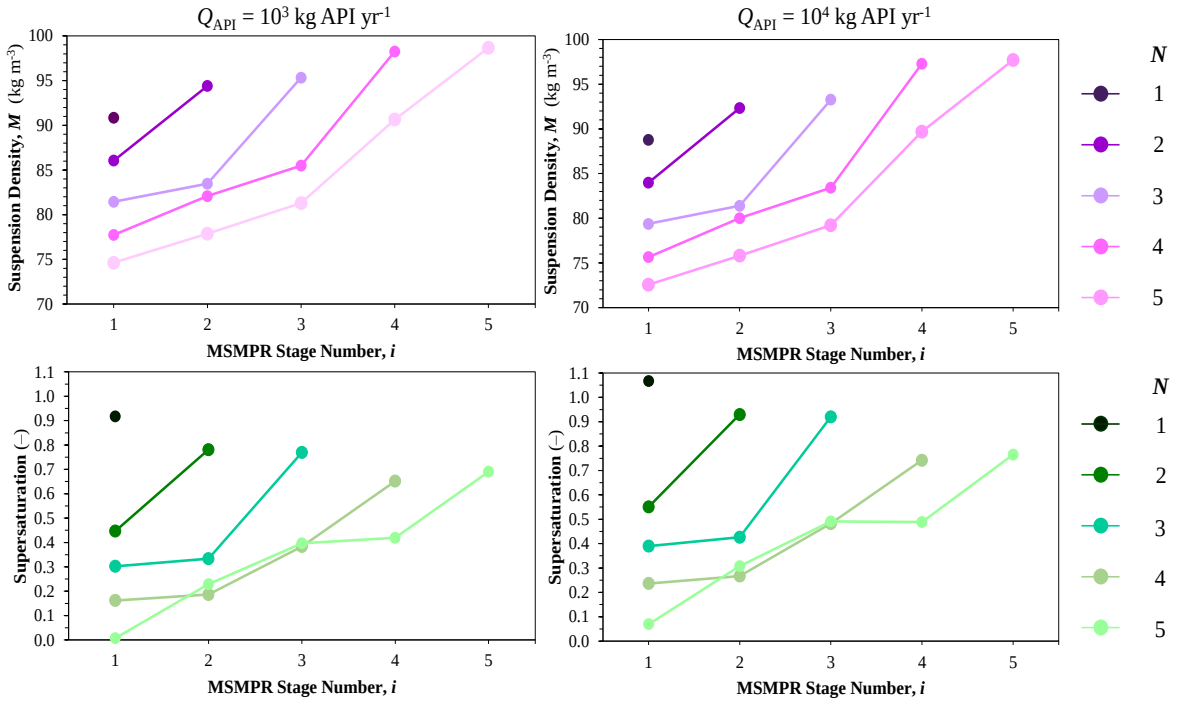

Figure 6: Optimal suspension densities (M) and supersaturations at both considered plant capacities (Q_{API}) at each stage (i) for different numbers of crystallizers (N).

The attained final *MCS* values for all cascade designs (implemented N) at different considered plant capacities (Q_{API}) are shown in Fig. 7. Values of *MCS* are slightly lower for the higher considered Q_{API}; the desired *MCS* depends on the implemented downstream unit operations and drug product formulation. The attained *MCS* values are low and will likely lead to difficulties in solid-liquid separation unit operation and flowability issues during downstream processes. This highlights a need to incorporate crystal quality (size properties as well as purity and polymorph constraints) into the problem formulation. The published nucleation and growth kinetic parameters from the literature that are used in this study did not account for agglomeration and breakage either, which will affect the computed crystal sizes. Harmonization of downstream unit operation design with the considered crystallization process, as well as upstream API synthesis, as part of plantwide design problems give significant insight into pharmaceutical process development where sufficient information for up- and downstream unit operation design is available.

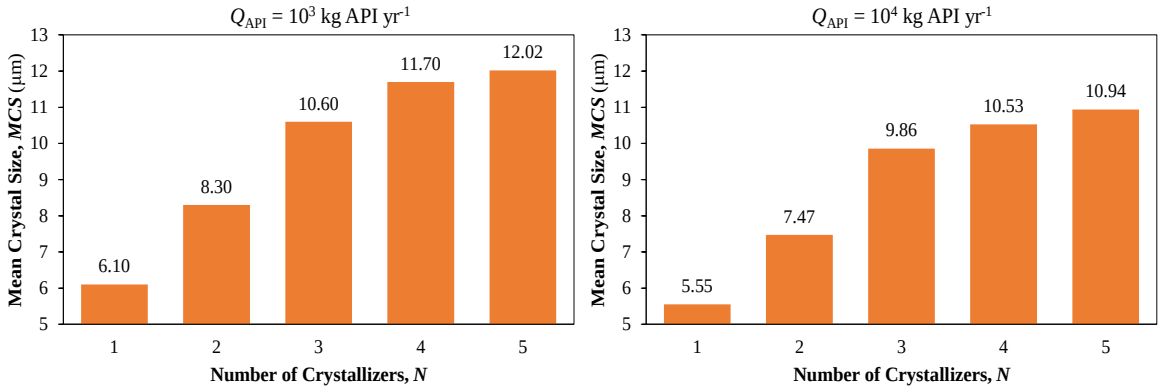

Figure 7: Final Mean Crystal Size (*MCS*) at both considered plant capacities (Q_{API}) for different assumed numbers of crystallizers (N).

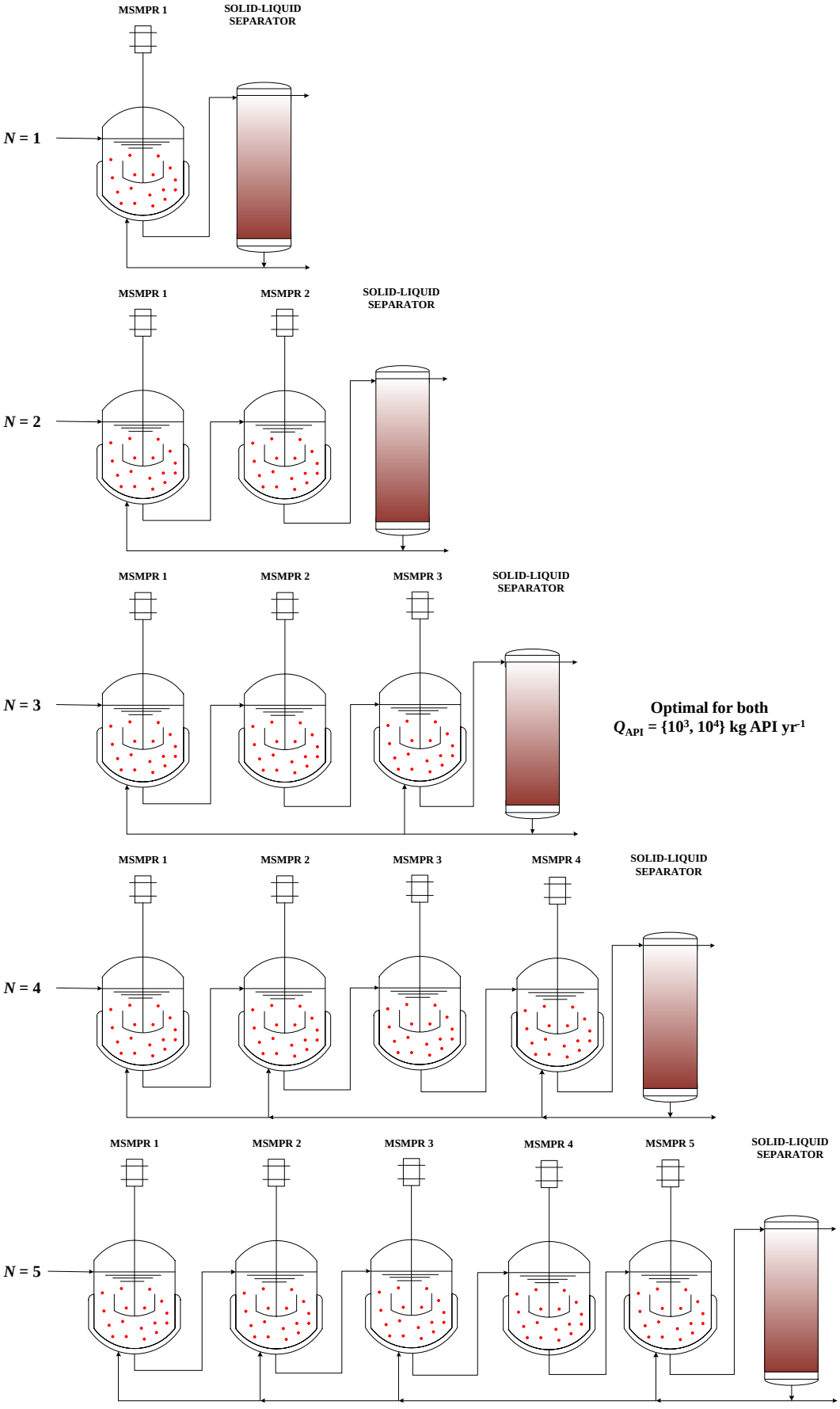

Figure 8: Optimal MSMPR cascade configurations for different numbers of crystallizers (N) at both considered plant capacities (Q_{API}).

Crystal breakage can occur in MSMPR crystallizers due to impeller and inter-particle collisions and turbulence within the crystallization magma. The considered population balance model and crystallization kinetics are that described by Capellades et al. (2018)[40], which does not explicitly consider breakage phenomena. The aim of the MINLP problem is for economic optimization of the MSMPR cascade to produce a specified mass of API crystalline annually (= plant capacity, Q_{API}). The problem constraints only pertain to crystallizer design + operation and annual API production and not to the product size properties; thus, consideration of breakage phenomena is unlikely to affect the computed *NPV* maxima presented in this study.

The chosen solution method of the population balance models is not expected to vary the computed *NPV*.[64] The population balance solution method is unlikely to drastically change the calculated yield, which affects the annual API production and thus process efficiency and *NPV*.

5.2 Optimal Flowsheet Designs

The optimal flowsheet configurations corresponding to MINLP optima (i.e., *NPV* maxima) are shown in Fig. 8. The optimal configurations presented in Fig. 8 (for both capacities) varies for different numbers of crystallizers (N). For $N = \{1,2\}$, recycle streams are allocated to all crystallizers in the MSMPR cascade. However, for $N \geq 3$, not all crystallizers have recycle streams fed to them, i.e., not all $y_i = 1$ (binary decision variable in the MINLP problem). Varying recycle flowrates to different crystallizers is important in controlling the crystallization yield and final crystalline product quality attributes. Lower capacities and effects of alternative numbers of crystallizers out with the range considered here (i.e., $N > 5$) can be easily investigated in the described MINLP optimization framework.

The optimal number of crystallizers is the same for both considered plant capacities (Q_{API}), $N = 3$, as is the allocation of recycle streams, i.e., to the first and final (third) crystallizers with the second vessel receiving no recycle; this corresponds to MINLP binary decision variables $y = [1\ 0\ 1]$. Varying the extent of recycle to different crystallizers has been shown to be an important decision variable in controlling the crystallization yield in MSMPR cascades with solids recycle,[11,58] which in turn affects the productivity and costs to attain a specific plant capacity. Allocating solids recycle to multiple stages, as opposed to just one crystallizer, increases the extent of nucleation throughout the cascade which increases the final crystallization yield. Were the final *MCS* or size distribution considered as objective functions or constraints in the optimization problem, allocation and extent of solids recycle may vary, as crystal growth would be more important. Implementing multi-objective optimization on both crystallization yields and product quality attributes such as *MCS* and size distribution width is often implemented for dynamic optimization of batch and continuous processes.[65]

The optimal recycle ratios (RR_{TOT}, extent of recycle) and clear mother liquor removal ratios (x, controlling concentration of recycle streams) for the considered plant capacities (Q_{API}) and numbers of crystallizers (N) are shown in Fig. 9. For both considered capacities, the optimal recycle ratios decrease from $N = 1$–3 and then increase, whereas the optimal clear mother liquor removal ratio decrease. Increasing RR_{TOT} and x increase the available surface area for crystallization in each vessel, however, ultimately incur greater recycle flowrates which require larger vessels (i.e., sufficient crystallizer residence time) to attain suitable yields and the desired productivity to meet the set capacity (Q_{API}). The decrease in the clear mother liquor removal ratio (x) from $N = 1$–3 indicates that the recycle streams do not need to be as concentrated (i.e., less mother liquor removed in waste stream F_{2N+2}) for $N = 3$ in order to be cost optimal; this also leads to less waste and enhanced material efficiency.

This study formulates a MINLP problem for *NPV* maximization of a MSMPR crystallization cascade with solids recycle. The current MINLP formulation assumes solids recycle streams are distributed equally between those crystallizers for which $y = 1$. An equal distribution of recycle streams has been considered for process simplification. The total recycle ratio (RR_{TOT}) is a continuous decision variable while the allocation of recycle to a crystallizer is described by the binary variable, $y_i = \{0,1\}$. This model framework allows one to optimize crystallizer design and operation as well as recycle allocation for a given number of crystallizers and specified plant capacity, under the assumption of equal distribution of recycle flowrate to multiple crystallizers. The current MINLP problem formulated for economic optimization does not consider product quality attribute constraints; however, were such constraints implemented, unequal recycle allocation may be beneficial.

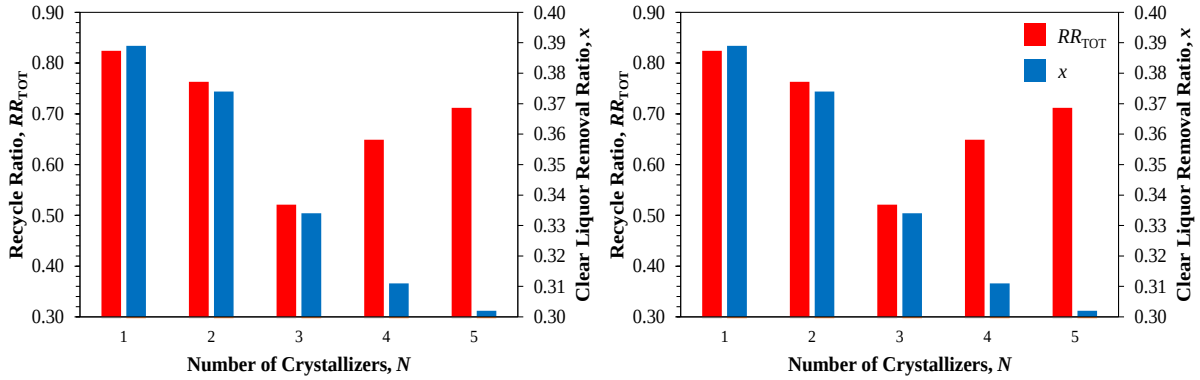

Figure 9: Optimal recycle ratios (RR_{TOT}) and clear mother liquor removal ratios (x) at both considered plant capacities (Q_{API}) at each stage (i) for different numbers of crystallizers (N).

Optimal crystallizer volumes (V) for different plant capacities (Q_{API}) and number of crystallizers (N) are shown in Fig. 10. As the number of implemented crystallizers increases from N = 1–3, total cascade volumes decrease and then increase for N > 3. As N increases, individual vessel volumes decrease; implementing multiple smaller volume stages is beneficial in terms of attained crystallization yield (see section 5.3, Fig. 11). Crystallizer volumes are larger for designs at the higher considered capacity, reflecting the larger volumetric throughputs to meet the higher API production requirements. While the optimal crystallizer volumes are computed to the millilitre; in industrial practice, it is likely that one will be using already constructed vessels with set fill volumes with incremental applicable fill volumes. However, this would require describing vessel volumes as discrete variables in the MINLP formulation, which presents an unnecessary level of problem complexity. Nevertheless, the optimization results presented here are strongly indicative of promising process configurations for *NPV* optimality for melitracen continuous crystallization in MSMPRs.

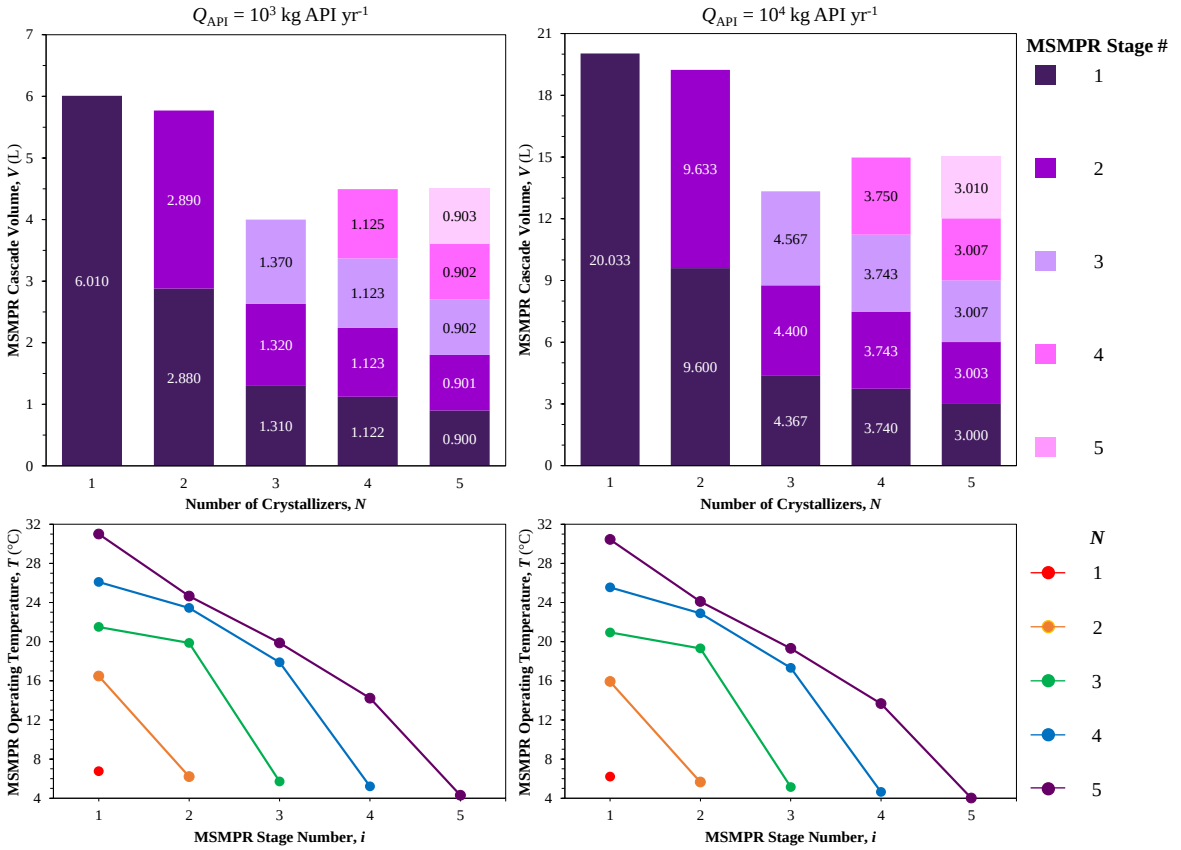

Figure 10: Optimal tank volumes (V) and MSMPR operating temperatures (T) at both considered plant capacities (Q_{API}) at each stage (i) for different numbers of crystallizers (N).

Optimal crystallizer operating temperatures (T) for different plant capacities (Q_{API}) and numbers of crystallizers (N) are also shown in Fig. 10. As N increases, individual stage temperatures are higher but the final temperature (T_N) is lower, which allows for increased crystallization yields.[36] Temperatures always decrease along the cascade to ensure supersaturation is generated in each crystallizer to cause more product API to crystallize from solution from the previous vessel, as imposed as one of the MINLP problem constraints (eq. 16). Implementation of Process Analytical Technology (PAT) is essential to ensure optimal temperatures are maintained. An assumption of the considered MSMPR model is that perfect mixing of the crystallizer contents is attained, such that the outlet solution concentration is the same as that throughout the MSMPR vessel. The model also assumes that heat transfer from crystallizer to cooling jacket is instant; the validity of this assumption decreases with increasing plant capacity and vessel volumes. Consideration of heat transfer dynamics can be considered as part of further non-steady-state studies.

5.3 Crystallization Yield and Plantwide Efficiencies

Attained crystallization yields (Y^{cryst}) at each MSMPR stage for different considered plant capacities (Q_{API}) and varying total numbers of crystallizers (N) are shown in Fig. 11. Yields progressively increase along the cascade as more API is crystallized from solution. Individual stage yields are lower as N increases, but ultimately the final yield increases when N is higher; eventually the final yield plateaus for $N \geq 4$. This indicates that beyond a certain number of crystallizers, the benefit of increasing yield with increasing N no longer becomes beneficial with respect to maximizing NPV.

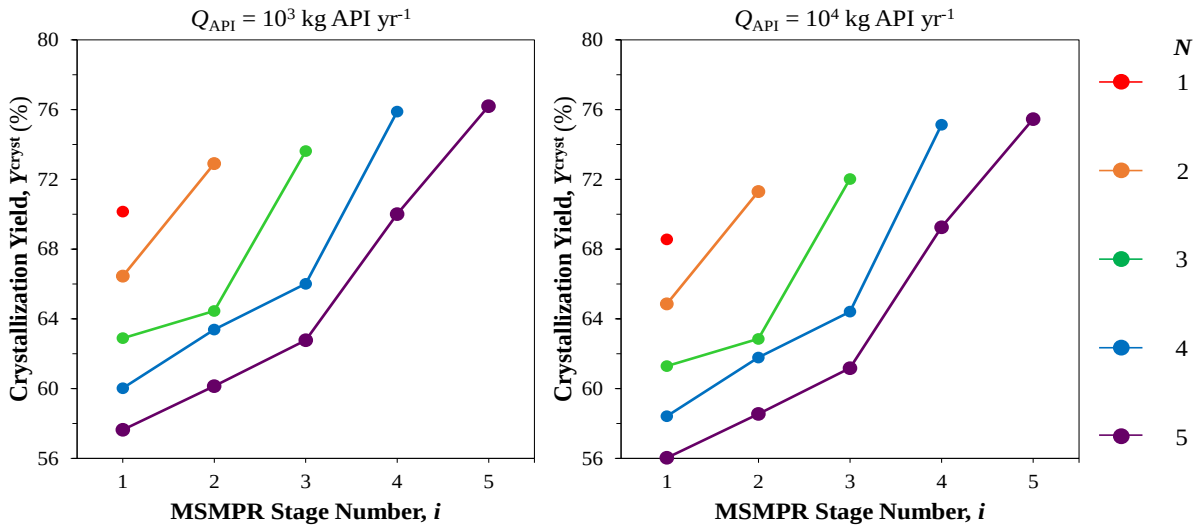

Figure 11: Optimal crystallization yields (Y^{cryst}) at both considered plant capacities (Q_{API}) at each stage (i) for different numbers of crystallizers (N).

Fig. 12 shows the mass flowrates of key flowsheet streams (see Fig. 2) corresponding to NPV maxima for different plant capacities (Q_{API}) and numbers of crystallizers (N). This analysis serves as a comparative evaluation of the amount of crystallized API withdrawn as product vs. that leaving the MSMPR cascade as waste and within recycle streams (R_i) + crystallizer holdups (HD_i). Detailed values of the data presented in Fig. 12 is presented in Table S1 in the Supplementary Information. The amount of crystallized API product (PR) for different numbers of crystallizers (N) is the same for different capacities, as each design must produce its target amount of API product. Total mass quantities differ between each capacity, reflecting the different total material throughputs required. For each considered capacity, there are similar trends observed. As the number of crystallizers (N) increases, the values of individual mass holdups and recycle streams decrease as the crystallization yields increase and the units become more efficient. However, the total material quantities decrease to a point (N = 3), i.e., the plant becomes more materially efficient, beyond which the total material quantities increase and the benefits of increasing N are no longer observed. The benefits of improving material efficiency with increasing N = 1–3 is also shown by the decreasing waste; for N > 3, the benefits of reduced waste decreases.

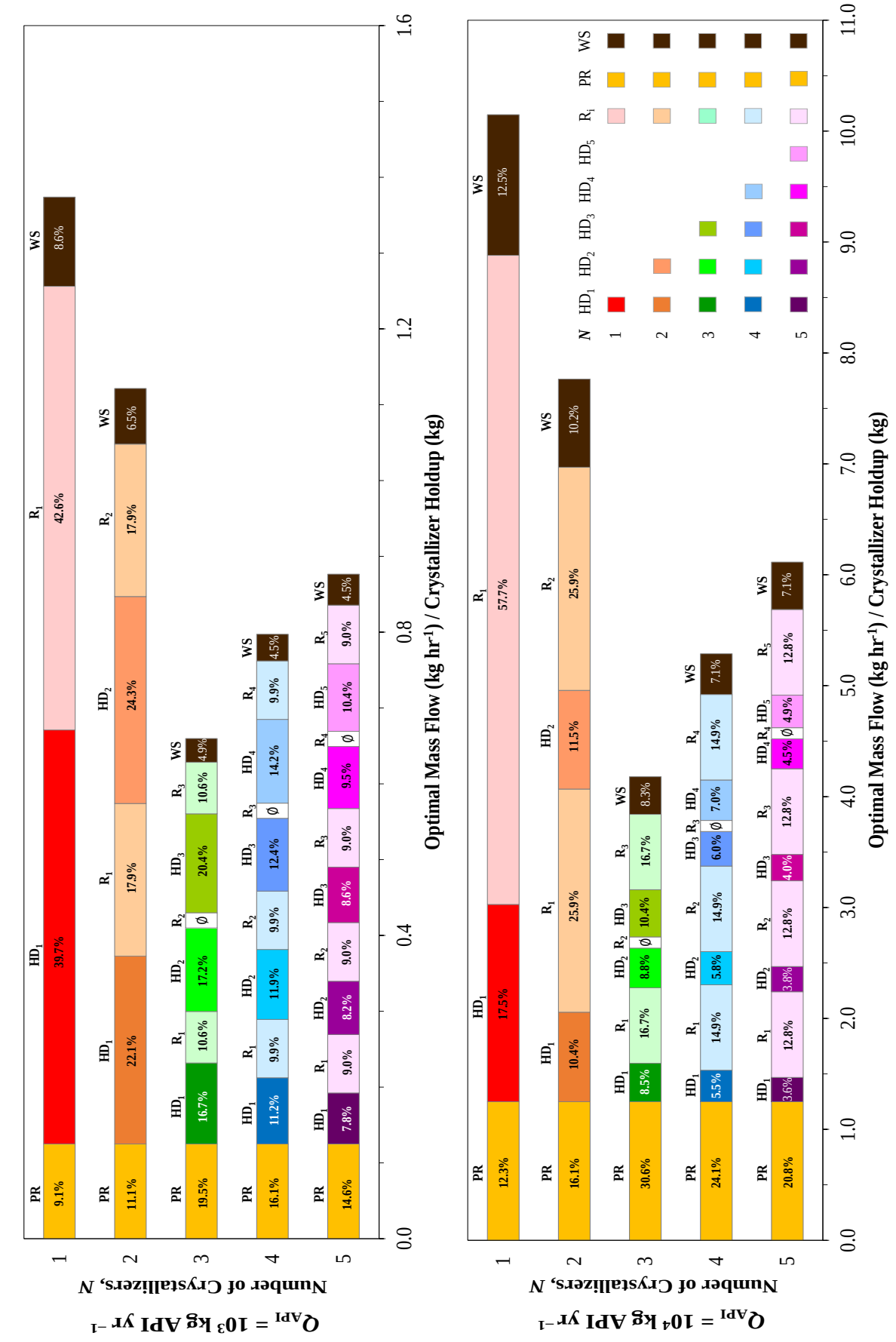

Figure 12: Optimal plantwide and MSMPR crystallizer mass holdups and flowrates of crystallized API in key flowsheet streams.

For both considered capacities, there are recycle streams which equal zero, i.e., the MINLP optimization problem has determined that no recycle be allocated to certain crystallizers (i.e., $y_i = 0$ for certain stages i). For the higher plant capacity ($Q_{API} = 10^4$ kg API yr^{-1}), relative quantities of product vs. API in recycle streams and vessel holdups is higher than at the lower capacity ($Q_{API} = 10^3$ kg API yr^{-1}); relative quantities of waste also increase.

The current study considers only a stream of pure melitracen in solution which is to be crystallized in the MSMPR cascade. Incorporation of impurities will require purge streams to prevent impurity accumulation as well as knowledge of partitioning of different impurity components between crystalline and solution phases. Recent studies considering the effects of impurity compounds on component solubilities and crystallization kinetics highlight the importance of such considerations.[66] While thermal degradation of melitracen was not reported within the considered temperature range in the experimental study from which crystallization kinetic parameters were taken,[40] expansion of this modelling framework to other APIs should take such phenomena and effects into consideration, as investigated in recent MSMPR studies.[67] Alternate capacities and effects of different numbers of crystallizers out with the range considered here (i.e., $N > 5$) can be easily investigated in the described MINLP framework, however the number of variables, constraints and computational time will increase substantially.

5.4 Economic Analysis

5.4.1 Net Present Value (NPV) Maxima and Total Cost Components

Optimal Capital (*CapEx*) and Operating (*OpEx*) Expenditure components for different plant capacities (Q_{API}) and number of implemented crystallizers (N) at the end of the plant lifetime are shown in Fig. 13. Total cost components are higher for $Q_{API} = 10^4$ kg API yr^{-1} than for 10^3 kg API yr^{-1} in correspondence with the required larger equipment and material throughputs for higher plant capacities. Total *CapEx* and *OpEx* components both decrease from $N = 1$–3 and then increase for $N > 3$, following the trend observed for cascade volumes (Fig. 10). This result is observed for *CapEx* components because *BLIC* is a function of equipment capacities (from *FOB* components), of which MSMPR vessels are a significant contributor; the sum of *WC* and *CC* components (= *WCC* in Fig. 13) is a function of material throughput (eq. 27), which also follows the same trend.

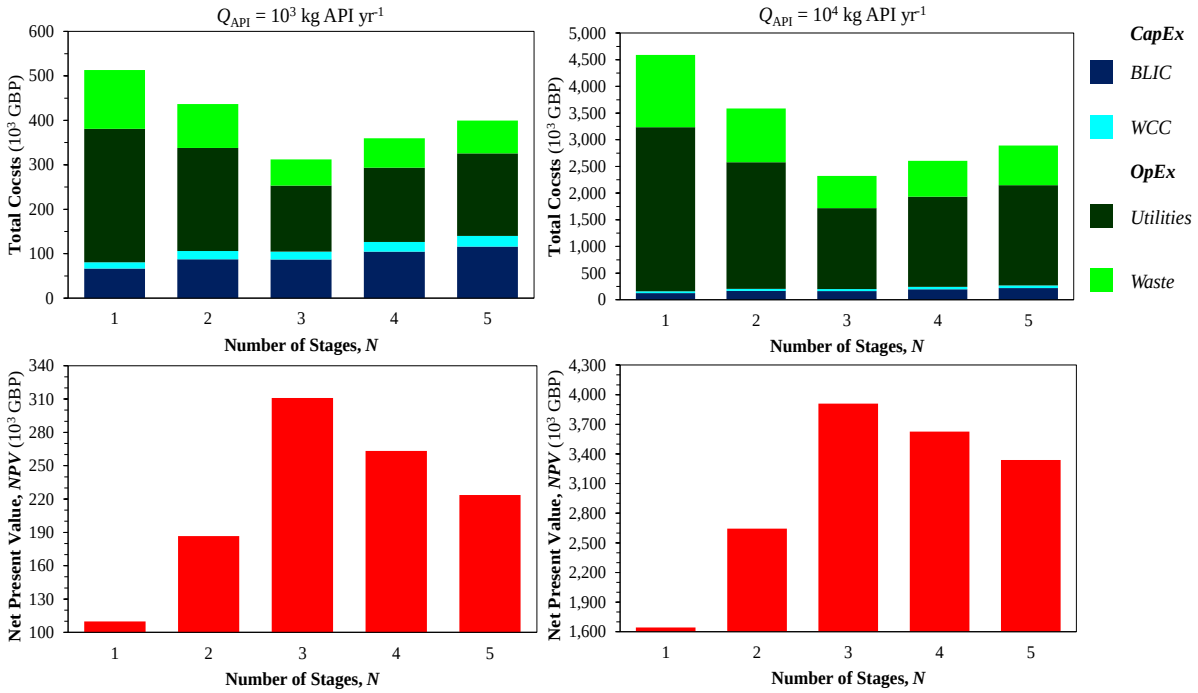

Figure 13: Optimal Capital (*CapEx*) and Operating (*OpEx*) Expenditure components and Net Present Values (*NPV*) at both considered plant capacities (Q_{API}) for different numbers of crystallizers (N).

Total *CapEx* is dominated by *BLIC* due to the costs of equipment being much greater than *WCC* costs which are a function of material throughputs (see Table 2). Total *OpEx* is dominated by utilities components, which are associated with material handling and MSMPR cooling (eq. 30). Solvent (i.e., ethanol from the mother liquor solution) recovery from product and waste streams (i.e., F_{2N+3} and F_{2N+2} in Fig. 2, respectively) is not considered but can easily be incorporated into the existing MINLP optimization framework.

Resulting *NPV* maxima for different plant capacities (Q_{API}) and numbers of implemented crystallizers (N) are also shown in Fig. 13. For both considered capacities, *NPV* maxima are attained for $N = 3$, where total cost components are their lowest. A previous NLP study of MSMPR cascade optimization without recycle for three different APIs showed that the optimal number of MSMPR crystallizers in a cascade for total cost minimization is dependent on plant capacity.[36] The optimal flowsheet configuration and crystallizer vessel design and operating parameters depend on the kinetic and thermodynamic (i.e., solubility) behaviour of the API being crystallized, the solvent in which the API is dissolved and the method of supersaturation generation; a recent study showed the importance of the solvent effect considerations on crystallization kinetics.[68] Nevertheless, given crystallization kinetic parameters and solubility behaviour, the current modelling framework may be expanded to other APIs amenable to cooling crystallization in MSMPR cascades.

Fig. 14 compares a *CapEx* component breakdown per crystallization unit vs. annualized *OpEx* components (calculated as the sum of time discounted *OpEx* over the plant lifetime and averaged per year) and annualized profits from API sales (averaged in the same way); a similar plot of absolute total *CapEx* and *OpEx* vs. profits at the end of the plant lifetime is presented in Fig. S1 (see Supplementary Information), along with a detailed list of values in Fig. 14 presented in Table S2 (see Supplementary Information). Profits are substantially higher vs. expenditures (negative cash flows) for the higher plant capacity; this supports the previous discussion of the benefits of operating this MSMPR cascade at higher production capacities. The *BLIC* breakdown per unit crystallizer are approximately the same for each capacity and number of crystallizers.

5.4.2 Sensitivity Analysis: Varying Interest Rates

Sensitivity analysis on the considered value of interest rate (r) is implemented to investigate the effect of varying this economic parameter on designs. Here, we vary the interest rate for the optimized designs (for which the base value is $r = 5\%$) for different considered plant capacities (Q_{API}) and number of crystallizers (N). Fig. 15 shows the effect of varying interest rates, $r = \{2, 5, 8, 10\}\%$, on the calculated *NPV* for fixed, optimal designs established by solution of the MINLP problems for both considered plant capacities (Q_{API}). At both capacities, the assumed value of r affects the final *NPV* at the end of the plant lifetime significantly; as r increases, the *NPV* decreases due to the greater effect of inflation and thus decreasing time value of profits. The percentage difference in *NPV* by varying r at $Q_{API} = 10^4$ kg API yr^{-1} is less than for $Q_{API} = 10^3$ kg API yr^{-1}, i.e., operating at higher production capacities is more economically stable. It is important to note that this sensitivity analysis has been performed by varying r for fixed optimal plant designs from the MINLP optimization problem solution in which $r = 5\%$ is the assumed value; it is possible that solving the MINLP optimization problem for different values of r may result in different optimal plant configurations and crystallizer designs for the considered values of Q_{API} and N. Nevertheless, variation of the assumed interest rate r is of value to investigate the effect of parameters related to economic climate.

The sensitivity analysis of interest rate (r) demonstrates that elucidating parameters with the greatest impact on model predictions is a valuable exercise. The effect of varying the assumed interest rate, $r = \{2, 5, 8, 10\}\%$, results in large deviations in predicted *NPV* (–42.36% to +41.72% *NPV* for $Q_{API} = 10^3$ kg API yr^{-1}; –33.30% to +32.80% *NPV* for $Q_{API} = 10^4$ kg API yr^{-1}), showing that it is a key model parameter. Further analysis could investigate the effect of additional economic parameters (e.g., equipment and material prices, waste handling rates, etc.) as well as uncertainty in the underlying crystallization kinetic parameters vs. their reported experimental values.[40] This could provide further insight into the drivers for comparing the economic viability of MSMPR cascade designs and give impetus to further optimization studies addressing parametric uncertainty; however, a full global systems analysis is out with the scope of this study.

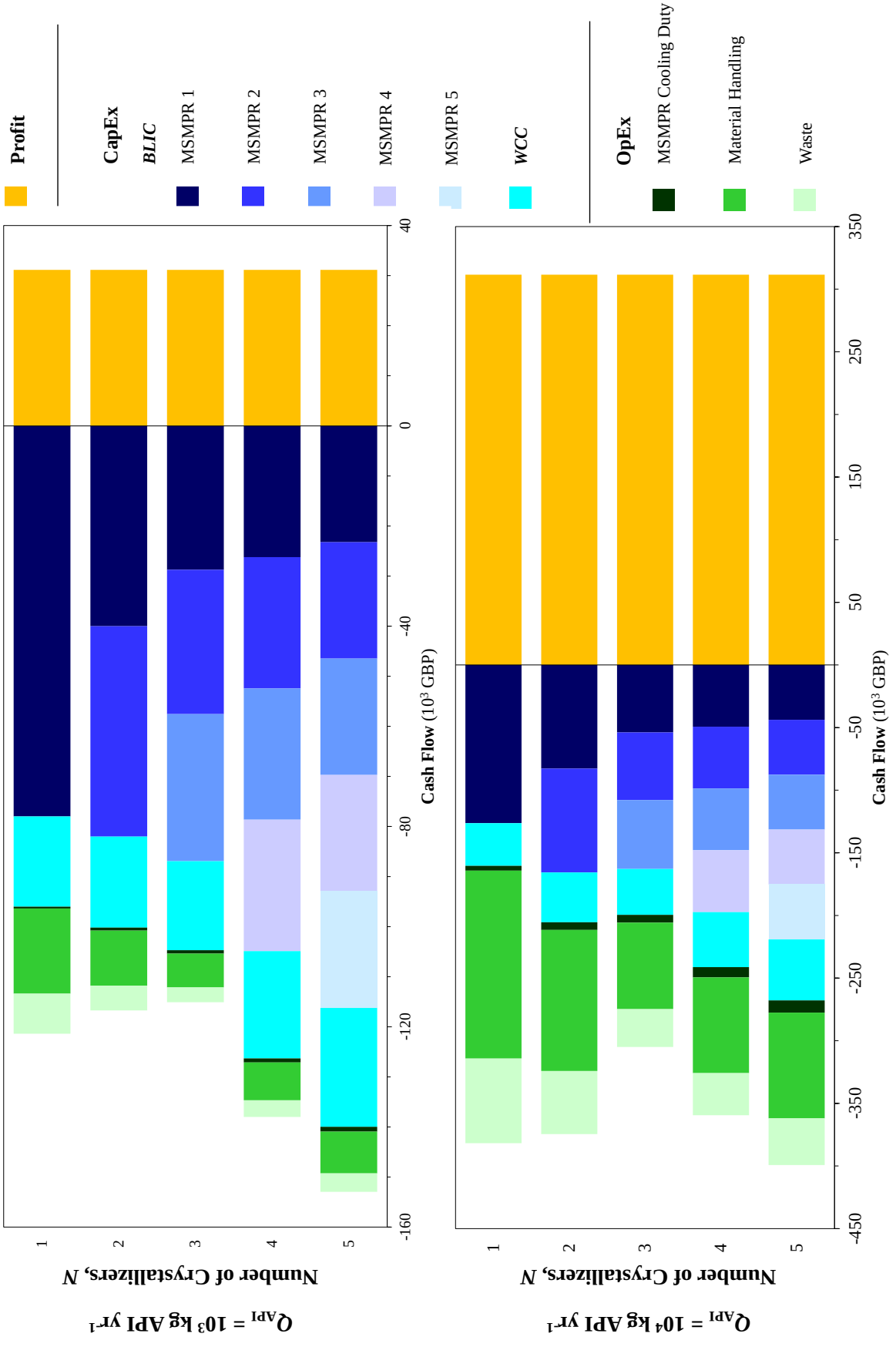

Figure 14: Annualized cost breakdown of cash flows for different considered plant capacities (Q_{API}) and numbers of crystallizers (N).

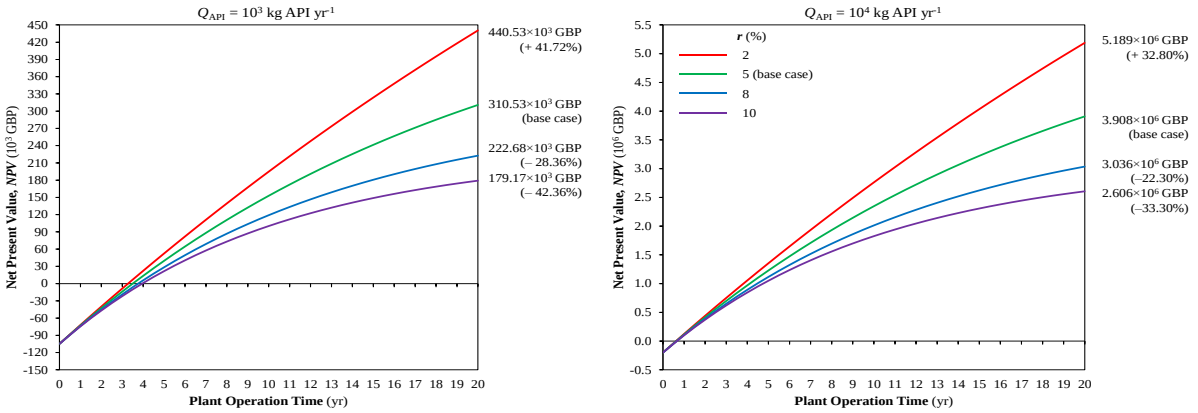

Figure 15: Net Present Value (*NPV*) vs. plant operation time for varying assumptions of interest rates (base case is r = 5%) for both considered plant capacities at their optimal plant designs (N = 3).

The Payback Period (*PBP*) is defined as the plant operation time taken for the total *CapEx* investment to be paid off, i.e., the time taken until *NPV* = 0. Calculated *PBP* for different plant capacities (Q_{API}), number of implemented crystallizers (N) and assumed interest rate (r) for optimal designs presented in previous sections are shown in Fig. 16. The calculated *PBP* values for $Q_{API} = 10^4$ kg API yr^{-1} are much less than for $Q_{API} = 10^3$ kg API yr^{-1}; while profits increase significantly at a higher capacity, total cost (i.e., *CapEx* and *OpEx* components) do not increase to have a detrimental effect on the economic performance. This result supports the idea that higher production capacities are beneficial for continuous crystallization. However, this does not account for the negative effects of scale on mixing and heat and mass transfer efficiencies, while the considered MSMPR model assumes perfect mixing.

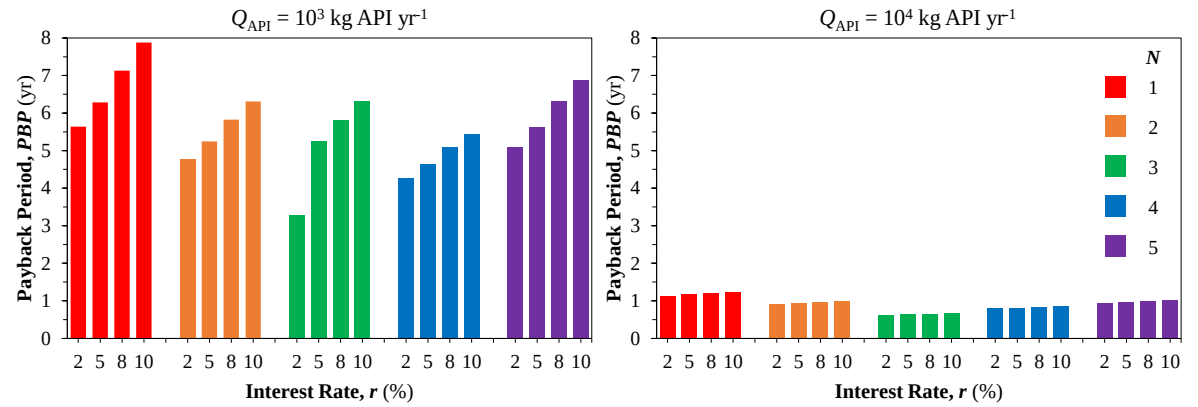

Figure 16: Payback Period (*PBP*) for varying assumptions of interest rates (base case r = 5%) for both considered plant capacities (Q_{API}) for different numbers of implemented crystallizers (N).

6. Conclusions

This study has constructed and solved a MINLP problem for the maximization of the Net Present Value of a cascade of continuous cooling MSMPR crystallizers for the production of melitracen. The MINLP optimization problem considered varying numbers of crystallizers (N = 1–5) and different plant API capacities ($Q_{API} = \{10^3, 10^4\}$ kg API yr^{-1}), with crystallizer vessel volumes, operating temperatures and recycle options as decision variables. Plantwide material efficiencies (i.e., crystallized API product vs. API withheld in the MSMPR cascade and lost in waste streams) increase until N = 3, beyond which the benefits of increasing the number of crystallizers decreases. The optimal number of vessels N = 3 for both considered capacities with recycle streams allocated to the first and third crystallizers. The final *NPV* values were shown to be sensitive to the considered interest rate. This study presents the first implementation of MINLP for the optimal design of a cascade of MSMPR crystallizers and its novelty and utility lie in the rapid screening of flowsheet configurations for pharmaceutical crystallization processes. The modelling and optimization framework can be extended to any API or solute amenable to cooling crystallization given the availability of kinetic parameters and solubility data.

Supplementary Information

Detailed process stream flowrates and cash flow components for optimal plant designs. This information is available free of charge via the Internet at http://pubs.acs.org/.

Author Information

Corresponding Author

Email: *D.Gerogiorgis@ed.ac.uk*
Phone: + *44 131 6517072*

Present Address

Samir Diab: Product & Process Engineering, GlaxoSmithKline Research & Development, Ware, UK.

ORCID

Samir Diab: 0000-0003-3476-2671
Dimitrios I. Gerogiorgis: 0000-0002-2210-6784

Acknowledgements

The authors gratefully acknowledge an Engineering and Physical Sciences Research Council (EPSRC) Doctoral Training Partnership (DTP) PhD Fellowship (Grant # EP/N509644/1) to Dr. Samir Diab, a Royal Society (RS) Short Fellowship (2020–2021) to Dr. Dimitrios I. Gerogiorgis and the Great Britain and Sasakawa Foundations. The authors declare no competing financial interest. Tabulated and cited literature data suffice for reproduction of all original process simulation and optimization results; no other supporting data are required for reproducibility.

Nomenclature and Acronyms

Acronyms

API	Active Pharmaceutical Ingredient
BONMIN	Basic Open-source Nonlinear Mixed Integer
CEPCI	Chemical Engineering Plant Cost Index
CPM	Continuous Pharmaceutical Manufacturing
DP	Drug Product
IPOPT	Interior Point Nonlinear Optimizer
LLE	Liquid-Liquid Extraction
MINLP	Mixed Integer Nonlinear Programme
NLP	Nonlinear Programme
PAT	Process Analytical Technology
PR	Product
WS	Waste

Variables

Latin Letters

b	Nucleation rate exponent in eq. 2 (–)
B_i	Nucleation rate in MSMPR i (# crystals m^{-3} suspension s^{-1})
BLIC	Battery Limits Installed Costs (GBP)
C_i	Equilibrium API concentrations in mother liquor of MSMPR i (kg API m^{-3} suspension)
C_i^{sat}	Solubility API concentrations in mother liquor of MSMPR i (kg API m^{-3} suspension)
C_0	Feed concentration of API solute in fresh mother liquor (kg API m^{-3} suspension)
CapEx	Capital Expenditure (GBP)
CC	Contingency Costs (GBP)
E_b	Energy barrier to nucleation (J mol^{-1})
E_g	Energy barrier to growth (J mol^{-1})
f	Correction factor in eq. 22 (–)
F_i	Volumetric flowrate of stream leaving MSMPR i (m^3 suspension s^{-1})

F_0	Volumetric flowrate of fresh feed entering the MSMPR cascade (m^3 suspension s^{-1})
FOB	Free-on-Board Costs (GBP)
g	Growth rate exponent in eq. 3 (–)
G_i	Growth rate in MSMPR i (m API s^{-1})
HD_i	Crystallizer API holdup in MSMPR i (kg API)
IEC	Installed Equipment Costs (GBP)
k_{b0}	Pre-exponential factor for nucleation (# crystals m^{-3} suspension s^{-1})
k_{g0}	Pre-exponential factor for growth (m API s^{-1})
k_v	API volume shape factor (–)
L	Crystal length (m API)
L_{av}	Average crystal length (m API)
m	Suspension density exponent in eq. 2 (–)
M_i	Suspension density in MSMPR i (kg API m^{-3} suspension)
MAT_{annual}	Annual material costs (GBP yr^{-1})
MCS	Mean Crystal Size (m API)
n	Exponent in eq. 22 (–)
N	Number of MSMPR crystallizers (–)
n_i	Crystal population density function (# crystals m^{-3} suspension m^{-1} API)
n_i^0	Nuclei population density function (# crystals m^{-3} suspension m^{-1} API)
NPV	Net Present Value (GBP)
$OpEx_{annual}$	Annual Operating Expenditure (GBP yr^{-1})
p_{API}	API wholesale price (GBP kg API^{-1})
P_j	Equipment purchase cost at capacity j (GBP)
PBP	Payback Period (yr)
PPI	Process Piping and Instrumentation Costs (GBP)
Q_{API}	Plant API capacity (kg API yr^{-1})
$Q_{MSMPR,i}$	Cooling duty for MSMPR i (kWh)
Q_{waste}	Volumetric flow of waste output (L waste yr^{-1})
r	Interest rate (%)
R	Universal gas constant (= 8.314 J mol^{-1} K^{-1})
R_i	Volumetric flowrate of recycle stream entering MSMPR i (m^3 suspension s^{-1})
R^2	Coefficient of determination (–)
RR_{TOT}	Total solids recycle ratio (–)
S_j	Capacity of equipment j (varying units – see Table 2)
t	Plant operation lifetime (yr)
T_i	Operating temperature of MSMPR i (°C)
$TPPC$	Total Physical Plant Cost (GBP)
$UTIL_{annual}$	Annual utilities costs (GBP yr^{-1})
V_i	Volume of MSMPR i (m^3 crystallizer)
$Waste_{annual}$	Annual waste disposal cost (GBP yr^{-1})
WC	Working Capital costs (GBP)
WCC	Working Capital + Contingency costs (GBP)
x	Clear mother liquor removal ratio in solid-liquid separation column (–)
y_i	Binary decision variable deciding whether to send recycle to MSMPR i (–)
Y_i^{cryst}	Crystallization yield in stage i (%)

Greek Letters

η	Electricity rate (GBP kWh^{-1})
ρ_{API}	API solid density (kg m^{-3} API)

References

(1) Wang, T.; Lu, H.; Wang, J.; Xiao, Y.; Zhou, Y.; Bao, Y.; Hao, H. Recent Progress of Continuous Crystallization. *J. Ind. Eng. Chem.* **2017**, *54*, 14–29.

(2) Baxendale, I. R.; Braatz, R. D.; Hodnett, B. K.; Jensen, K. F.; Johnson, M. D.; Sharratt, P.; Sherlock, J. P.; Florence, A. J. Achieving Continuous Manufacturing: Technologies and Approaches for Synthesis, Workup, and Isolation of Drug Substance May 20–21, 2014 Continuous Manufacturing Symposium. *J. Pharm. Sci.* **2015**, *104* (3), 781–791.

(3) Teoh, S. K.; Rathi, C.; Sharratt, P. Practical Assessment Methodology for Converting Fine Chemicals Processes from Batch to Continuous. *Org. Process Res. Dev.* **2015**, *20* (2), 414–431.

(4) Poechlauer, P.; Colberg, J.; Fisher, E.; Jansen, M.; Johnson, M. D.; Koenig, S. G.; Lawler, M.; Laporte, T.; Manley, J.; Martin, B.; O'Kearney-McMullan, A. Pharmaceutical Roundtable Study Demonstrates the Value of Continuous Manufacturing in the Design of Greener Processes. *Org. Process Res. Dev.* **2013**, *17* (12), 1472–1478.

(5) Chiu, T.; Christofides, P. D. Nonlinear Control of Particulate Processes. *AIChE J.* **1999**, *45* (6), 1279–1297.

(6) Chiu, T. Y.; Christofides, P. D. Robust Control of Particulate Processes Using Uncertain Population Balances. *AIChE J.* **2000**, *46* (2), 266–280.

(7) El-Farra, N. H.; Chiu, T. Y.; Christofides, P. D. Analysis and Control of Particulate Processes with Input Constraints. *AIChE J.* **2001**, *47* (8), 1849–1865.

(8) Su, Q.; Nagy, Z. K.; Rielly, C. D. Pharmaceutical Crystallisation Processes from Batch to Continuous Operation Using MSMPR Stages: Modelling, Design, and Control. *Chem. Eng. Process. Process Intensif.* **2015**, *89*, 41–53.

(9) Wood, B.; Girard, K. P.; Polster, C. S.; Croker, D. M. Progress to Date in the Design and Operation of Continuous Crystallization Processes for Pharmaceutical Applications. *Org. Process Res. Dev.* **2019**, *23* (2), 122–144.

(10) Ferguson, S.; Morris, G.; Hao, H.; Barrett, M.; Glennon, B. Characterization of the Anti-Solvent Batch, Plug Flow and MSMPR Crystallization of Benzoic Acid. *Chem. Eng. Sci.* **2013**, *104*, 44–54.

(11) Li, J.; Trout, B. L.; Myerson, A. S. Multistage Continuous Mixed-Suspension, Mixed-Product Removal (MSMPR) Crystallization with Solids Recycle. *Org. Process Res. Dev.* **2016**, *20* (2), 510–516.

(12) Park, K.; Kim, D. Y.; Yang, D. R. Operating Strategy for Continuous Multistage Mixed Suspension and Mixed Product Removal (MSMPR) Crystallization Processes Depending on Crystallization Kinetic Parameters. *Ind. Eng. Chem. Res.* **2016**, *55* (26), 7142–7153.

(13) Yang, Y.; Nagy, Z. K. Combined Cooling and Antisolvent Crystallization in Continuous Mixed Suspension, Mixed Product Removal Cascade Crystallizers: Steady-State and Startup Optimization. *Ind. Eng. Chem. Res.* **2015**, *54* (21), 5673–5682.

(14) Yang, Y.; Nagy, Z. K. Advanced Control Approaches for Combined Cooling/Antisolvent Crystallization in Continuous Mixed Suspension Mixed Product Removal Cascade Crystallizers. *Chem. Eng. Sci.* **2015**, *127*, 362–373.

(15) Vetter, T.; Burcham, C. L.; Doherty, M. F. Regions of Attainable Particle Sizes in Continuous and Batch Crystallization Processes. *Chem. Eng. Sci.* **2014**, *106*, 167–180.

(16) Acevedo, D.; Yang, Y.; Warnke, D. J.; Nagy, Z. K. Model-Based Evaluation of Direct Nucleation Control Approaches for the Continuous Cooling Crystallization of Paracetamol in a Mixed Suspension Mixed Product Removal System. *Cryst. Growth Des.* **2017**, *17* (10), 5377–5383.

(17) Yang, X.; Acevedo, D.; Mohammad, A.; Pavurala, N.; Wu, H.; Brayton, A. L.; Shaw, R. A.; Goldman, M. J.; He, F.; Li, S.; Fisher, R. J.; O'Connor, T. F.; Cruz, C. N. Risk Considerations on Developing a Continuous Crystallization System for Carbamazepine. *Org. Process Res. Dev.* **2017**, *21* (7), 1021–1033.

(18) Vetter, T.; Burcham, C. L.; Doherty, M. F. Designing Robust Crystallization Processes in the Presence of Parameter Uncertainty Using Attainable Regions. *Ind. Eng. Chem. Res.* **2015**, *54* (42), 10350–10363.

(19) Sang-Il Kwon, J.; Nayhouse, M.; Orkoulas, G.; Christofides, P. D. Crystal Shape and Size Control Using a Plug Flow Crystallization Configuration. *Chem. Eng. Sci.* **2014**, *119*, 30–39.

(20) Su, Q.; Rielly, C. D.; Powell, K. A.; Nagy, Z. K. Mathematical Modelling and Experimental Validation of a Novel Periodic Flow Crystallization Using MSMPR Crystallizers. *AIChE J.* **2017**, *63* (4), 1313–1327.

(21) Powell, K. A.; Saleemi, A. N.; Rielly, C. D.; Nagy, Z. K. Periodic Steady-State Flow Crystallization of a Pharmaceutical Drug Using MSMPR Operation. *Chem. Eng. Process. Process Intensif.* **2015**, *97*, 195–212.

(22) Tahara, K.; O'Mahony, M.; Myerson, A. S. Continuous Spherical Crystallization of Albuterol Sulfate with Solvent Recycle System. *Cryst. Growth Des.* **2015**, *15* (10), 5155–5156.

(23) Li, J.; Lai, T. C.; Trout, B. L.; Myerson, A. S. Continuous Crystallization of Cyclosporine: The Effect of Operating Conditions on Yield and Purity. *Cryst. Growth Des.* **2017**, *17* (3), 1000–1007.

(24) Vartak, S.; Myerson, A. S. Continuous Crystallization with Impurity Complexation and Nanofiltration Recycle. *Org. Process Res. Dev.* **2017**, *21* (2), 253–261.

(25) Hou, G.; Power, G.; Barrett, M.; Glennon, B.; Morris, G.; Zhao, Y. Development and Characterization of a Single Stage Mixed-Suspension, Mixed-Product-Removal Crystallization Process with a Novel Transfer Unit. *Cryst. Growth Des.* **2014**, *14* (4), 1782–1793.

(26) Acevedo, D.; Peña, R.; Yang, Y.; Barton, A.; Firth, P.; Nagy, Z. K. Evaluation of Mixed Suspension Mixed Product Removal Crystallization Processes Coupled with a Continuous Filtration System. *Chem. Eng. Process. Process Intensif.* **2016**, *108*, 212–219.

(27) Wang, J.; Lakerveld, R. Integrated Solvent and Process Design for Continuous Crystallization and Solvent Recycling Using PC-SAFT. *AIChE J.* **2018**, *64* (4), 1205–1216.

(28) Galan, K.; Eicke, M. J.; Elsner, M. P.; Lorenz, H.; Seidel-Morgenstern, A. Continuous Preferential Crystallization of Chiral Molecules in Single and Coupled Mixed-Suspension Mixed-Product-Removal Crystallizers. *Cryst. Growth Des.* **2015**, *15* (4), 1808–1818.

(29) Sang-Il Kwon, J.; Nayhouse, M.; Christofides, P. D.; Orkoulas, G. Modeling and Control of Crystal Shape in Continuous Protein Crystallization. *Chem. Eng. Sci.* **2014**, *107*, 47–57.

(30) Vetter, T.; Burcham, C. L.; Doherty, M. F. Separation of Conglomerate Forming Enantiomers Using a Novel Continuous Preferential Crystallization Process. *AIChE J.* **2015**, *61* (9), 2810–2823.

(31) Lai, T.-T. C.; Cornevin, J.; Ferguson, S.; Li, N.; Trout, B. L.; Myerson, A. S. Control of Polymorphism in Continuous Crystallization via Mixed Suspension Mixed Product Removal Systems Cascade Design. *Cryst. Growth Des.* **2015**, *15* (7), 3374–3382.

(32) Lai, T. T. C.; Ferguson, S.; Palmer, L.; Trout, B. L.; Myerson, A. S. Continuous Crystallization and Polymorph Dynamics in the L-Glutamic Acid System. *Org. Process Res. Dev.* **2014**, *18* (11), 1382–1390.

(33) Yang, Y.; Song, L.; Gao, T.; Nagy, Z. K. Integrated Upstream and Downstream Application of Wet Milling with Continuous Mixed Suspension Mixed Product Removal Crystallization. *Cryst. Growth Des.* **2015**, *15* (12), 5879–5885.

(34) Li, Y.; O'Shea, S.; Yin, Q.; Vetter, T. Polymorph Selection by Continuous Crystallization in the Presence of Wet Milling. *Cryst. Growth Des.* **2019**, *19* (4), 2259–2271.

(35) Li, H.; Yang, B. S. Model Evaluation of Particle Breakage Facilitated Process Intensification for Mixed-Suspension-Mixed-Product-Removal (MSMPR) Crystallization. *Chem. Eng. Sci.* **2019**, *207*, 1175–1186.

(36) Diab, S.; Gerogiorgis, D. I. Technoeconomic Optimization of Continuous Crystallization for Three Active Pharmaceutical Ingredients (APIs): Cyclosporine, Paracetamol and Aliskiren. *Ind. Eng. Chem. Res.* **2018**, *57* (29), 9489–9499.

(37) Buschmann, H. *Antidepressants, Antipsychotics, Anxiolytics: From Chemistry and Pharmacology to Clinical Application*; Wiley-VCH: Weinheim; 2007.

(38) Ritchie, H.; Roser, M. Mental Health. *OurWorldInData* **2019**, 1500–1531.

(39) Organisation for Economic Co-operation and Development (OECD). Pharmaceutical Market https://stats.oecd.org/Index.aspx?DataSetCode=HEALTH_PHMC# (accessed Jul 3, 2019).

(40) Capellades, G.; Joshi, P. U.; Dam-Johansen, K.; Mealy, M. J.; Christensen, T. V.; Kiil, S. Characterization of a Multistage Continuous MSMPR Crystallization Process Assisted by Image Analysis of Elongated Crystals. *Cryst. Growth Des.* **2018**, *18* (11), 6455–6469.

(41) Jolliffe, H. G.; Gerogiorgis, D. I. Plantwide Design and Economic Evaluation of Two Continuous Pharmaceutical Manufacturing (CPM) Cases: Ibuprofen and Artemisinin. *Comput. Chem. Eng.* **2016**, *91* (1), 269–288.

(42) Jolliffe, H. G.; Gerogiorgis, D. I. Process Modelling, Design and Technoeconomic Evaluation for Continuous Paracetamol Crystallisation. *Comput. Chem. Eng.* **2018**, *118*, 224–235.

(43) Nadeem, Z.; Mcintosh, A.; Lawrie, S. Mental Health Mental Health. *OurWorldInData* **2004**, No. April, 1500–1531.

(44) Organisation for Economic Co-operation and Development (OECD). Pharmaceutical Market.

(45) Aggarwal, A.; Floudas, C. A. Synthesis of Heat Integrated Nonsharp Distillation Sequences. *Comput. Chem. Eng.* **1992**, *16* (2), 89–108.

(46) Novak, Z.; Kravanja, Z.; Grossmann, I. E. Simultaneous Synthesis of Distillation Sequences in Overall Process Schemes Using an Improved MINLP Approach. *Comput. Chem. Eng.* **1996**, *20* (12), 1425–1440.

(47) Franke, M. B. Design of Dividing-Wall Columns by Mixed-Integer Nonlinear Programming Optimization. *Chemie Ing. Tech.* **2017**, *89* (5), 582–597.

(48) Smith, O. J.; Westerberg, A. W. The Optimal Design of Pressure Swing Adsorption Systems. *Chem. Eng. Sci.* **1991**, *46* (12), 2967–2976.

(49) Al Wahedi, Y.; Rabie, A. H.; Al Shaiba, A.; Geuzebroek, F.; Daoutidis, P. Optimization of Adsorption-Based Natural Gas Dryers. *Ind. Eng. Chem. Res.* **2016**, *55* (16), 4658–4667.

(50) Alonso, A. I.; Lassahn, A.; Gruhn, G. Optimal Design of Non-Dispersive Solvent Extraction Processes. *Comput. Chem. Eng.* **2001**, *25* (2–3), 267–285.

(51) Diab, S.; Gerogiorgis, D. I. Technoeconomic Mixed Integer Nonlinear Programming (MINLP) Optimization for Design of Liquid-Liquid Extraction (LLE) Cascades in Continuous Pharmaceutical Manufacturing of Atropine. *AIChE J.* **2019**, *65* (11), e16738.

(52) Emet, S.; Westerlund, T. Comparisons of Solving a Chromatographic Separation Problem Using MINLP Methods. *Comput. Chem. Eng.* **2004**, *28* (5), 673–682.

(53) Kanchanalai, P.; Lively, R. P.; Realff, M. J.; Kawajiri, Y. Cost and Energy Savings Using an Optimal Design of Reverse Osmosis Membrane Pretreatment for Dilute Bioethanol Purification. *Ind. Eng. Chem. Res.* **2013**, *52* (32), 11132–11141.

(54) Tsiakis, P.; Papageorgiou, L. G. Optimal Design of an Electrodialysis Brackish Water Desalination Plant. *Desalination* **2005**, *173* (2), 173–186.

(55) Aliaga-Vicente, A.; Caballero, J. A.; Fernández-Torres, M. J. Synthesis and Optimization of Membrane Cascade for Gas Separation via Mixed-Integer Nonlinear Programming. *AIChE J.* **2017**, *63* (6), 1989–2006.

(56) Ridder, B. J.; Majumder, A.; Nagy, Z. K. Population Balance Model-Based Multiobjective Optimization of a Multisegment Multiaddition (MSMA) Continuous Plug-Flow Antisolvent Crystallizer. *Ind. Eng. Chem. Res.* **2014**, *53* (11), 4387–4397.

(57) Su, Q.; Benyahia, B.; Nagy, Z. K.; Rielly, C. D. Mathematical Modeling, Design, and Optimization of a Multisegment Multiaddition Plug-Flow Crystallizer for Antisolvent Crystallizations. *Org. Process Res. Dev.* **2015**, *19*, 1859–1870.

(58) Diab, S.; Gerogiorgis, D. I. Technoeconomic Evaluation of Multiple Mixed Suspension-Mixed Product Removal (MSMPR) Crystallizer Configurations for Continuous Cyclosporine Crystallization. *Org. Process Res. Dev.* **2017**, *21* (10), 1571–1587.

(59) Morris, G.; Power, G.; Ferguson, S.; Barrett, M.; Hou, G.; Glennon, B. Estimation of Nucleation and Growth Kinetics of Benzoic Acid by Population Balance Modeling of a Continuous Cooling Mixed Suspension, Mixed Product Removal Crystallizer. *Org. Process Res. Dev.* **2015**, *19* (12), 1891–1902.

(60) Woods, D. R. *Rules of Thumb in Engineering Practice*; Wiley-VCH: Weinheim; 2007.

(61) Couper, J. R. *Process Engineering Economics*; CRC Press: Boca Raton; 2003.

(62) Bonami, P.; Biegler, L. T.; Conn, A. R.; Cornuéjols, G.; Grossmann, I. E.; Laird, C. D.; Lee, J.; Lodi, A.; Margot, F.; Sawaya, N.; Wächter, A. An Algorithmic Framework for Convex Mixed Integer Nonlinear Programs. *Discret. Optim.* **2008**, *5* (2), 186–204.

(63) Wächter, A.; Biegler, L. T. On the Implementation of an Interior-Point Filter Line-Search Algorithm for Large-Scale Nonlinear Programming. *Math. Program.* **2006**, *106* (1), 25–57.

(64) Omar, H. M.; Rohani, S. Crystal Population Balance Formulation and Solution Methods: A Review. *Cryst. Growth Des.* **2017**, *17*, 4028–4041

(65) Dafnomilis, A.; Diab, S.; Rodman, A. D.; Boudouvis, A. G.; Gerogiorgis, D. I. Multi-Objective Dynamic Optimization of Ampicillin Batch Crystallization: Sensitivity Analysis of Attainable Performance vs. Product Quality Constraints. *Ind. Eng. Chem. Res.* **2019**, *58* (40), 18756–18771.

(66) Capellades, G.; Wiemeyer, H.; Myerson, A. S. Mixed-Suspension, Mixed-Product Removal Studies of Ciprofloxacin from Pure and Crude Active Pharmaceutical Ingredients: The Role of Impurities on Solubility and Kinetics. *Cryst. Growth Des.* **2019**, *19* (7), 4008–4018.

(67) Pal, K.; Yang, Y.; Nagy, Z. K. Model-Based Optimization of Cooling Crystallization of Active Pharmaceutical Ingredients Undergoing Thermal Degradation. *Cryst. Growth Des.* **2019**, *19* (6), 3417–3429.

(68) Schall, J. M.; Mandur, J. S.; Braatz, R. D.; Myerson, A. S. Nucleation and Growth Kinetics for Combined Cooling and Antisolvent Crystallization in a Mixed-Suspension, Mixed-Product Removal System: Estimating Solvent Dependency. *Cryst. Growth Des.* **2018**, *18* (3), 1560–1570.